NASA TECHNICAL NOTE

NASA TN D-3642

NASA TN D-3642

THERMAL DESIGN EVALUATION OF PEGASUS

by Roger Linton

George C. Marshall Space Flight Center

Huntsville, Ala.

NATIONAL AERONAUTICS AND SPACE ADMINISTRATION • WASHINGTON, D. C. • DECEMBER 1966

NASA TN D-3642

THERMAL DESIGN EVALUATION OF PEGASUS

By Roger Linton

George C. Marshall Space Flight Center
Huntsville, Ala.

NATIONAL AERONAUTICS AND SPACE ADMINISTRATION

For sale by the Clearinghouse for Federal Scientific and Technical Information
Springfield, Virginia 22151 – Price $2.00

TABLE OF CONTENTS

LIST OF ILLUSTRATIONS

LIST OF ILLUSTRATIONS (Concluded)

LIST OF TABLES

THERMAL DESIGN EVALUATION OF PEGASUS

SUMMARY

Certain aspects of spacecraft thermal design often involve an artful approximation. Theoretical and experimental procedures can closely simulate the expected orbital conditions, but the exact thermal environment for an extended satellite lifetime is not wholly predictable. As a result, an evaluation of the Pegasus thermal design, based on telemetered temperature data, should illuminate several problem areas and aid in the improvement of thermal design techniques. The methods and results of the thermal design evaluation of Pegasus are the subjects of this report.

Three particular areas were selected for this analysis: (1) the micrometeoroid detector panels, (2) the louver system, and (3) the service module adaptor. Results indicate that the thermal design of the three Pegasus spacecraft was successful and adequate in most respects. A significant part of this success was, however, due to the small eccentricity of the satellite orbits. The thermal design was accomplished on the assumption of a highly eccentric orbit with a T_x (per cent time in sunlight) approaching 90 per cent ; a more circular orbit was eventually chosen, too late for thermal design changes, with a correspondingly lower value of T_x. It is apparent, upon studying post-launch temperature data, that the effect of this change was to maintain the Pegasus temperature more closely within the designed tolerances.

INTRODUCTION

The Pegasus satellite was conceived and developed as a means of further defining the micrometeoroid hazards to manned space flight. A series of three satellites, designated Pegasus I, II, and III, were launched on February 16, May 25, and July 30, 1965, respectively. Mission lifetime was expected to be one year for each satellite, during which time, it was presumed, sufficient micrometeoroid statistical data would be compiled with which to predict puncture frequency for near-earth orbits.

The thermal design of a Pegasus satellite was essential for the one-year expected lifetime. This included maintaining the various components of the spacecraft within prescribed temperature limits and preventing damaging thermal fluctuations.

Pegasus employs both active and passive thermal control. The active thermal control system was represented by the louver array at the base of the electronics canister. Passive thermal control by means of thin exterior coatings with desirable radiometric properties was employed on nearly every surface of the Pegasus satellite, including the upper stages of the attached Saturn launch vehicle. The Space Thermodynamics Branch (R-RP-T) of Research Projects Laboratory was responsible for the Pegasus thermal design [1]. Thermal design evaluation was made to determine the effectiveness of the active and passive thermal control mechanisms; this involved studies of the degradation of thermal control coatings used on the service module adaptor (SMA) and the meteoroid detector panels, generation of calculated temperatures from heat balance analysis, comparison of predicted and actual temperatures, and evaluation of the active control louvers on the electronics canister.

TEMPERATURE MEASUREMENTS OF PEGASUS

Twenty-five temperature probes were included on each Pegasus satellite to monitor system thermal status and to provide input for the thermal design evaluation. The temperature data are transmitted by two different modes of telemetry. Nineteen probes are of the pulse amplitude modulated (PAM) variety, while the remaining six are pulse code modulated (PCM). PAM data are transmitted continuously with a 15-second period of repetition; however, reception is limited to those intervals the spacecraft remains within the field of view of a tracking station (about 15 minutes). Initially, several stations tracked each Pegasus orbit for about two weeks. Thereafter, only one pass per orbit was tracked.

PCM data are stored in a core memory on board the satellite and are transmitted rapidly in toto upon ground command. Two of these digitized temperature probes are located on the opposite faces of a dummy meteoroid detector panel. The remaining digitized temperature measuring devices, located on special surfaces designed to study, experimentally, the radiometric properties of the Pegasus thermal control coatings, supply data for a thermal control coatings experiment [2].

There are nine PAM temperature probes on the temperature-sensitive components inside the electronics canister, two probes on the radiation detector package, a temperature probe on each of the four solar cell panels, three probes on the SMA skin, and a probe on the container of the thermal control coatings experiment. (An example of one of the temperature probes is shown in Figure 1.)

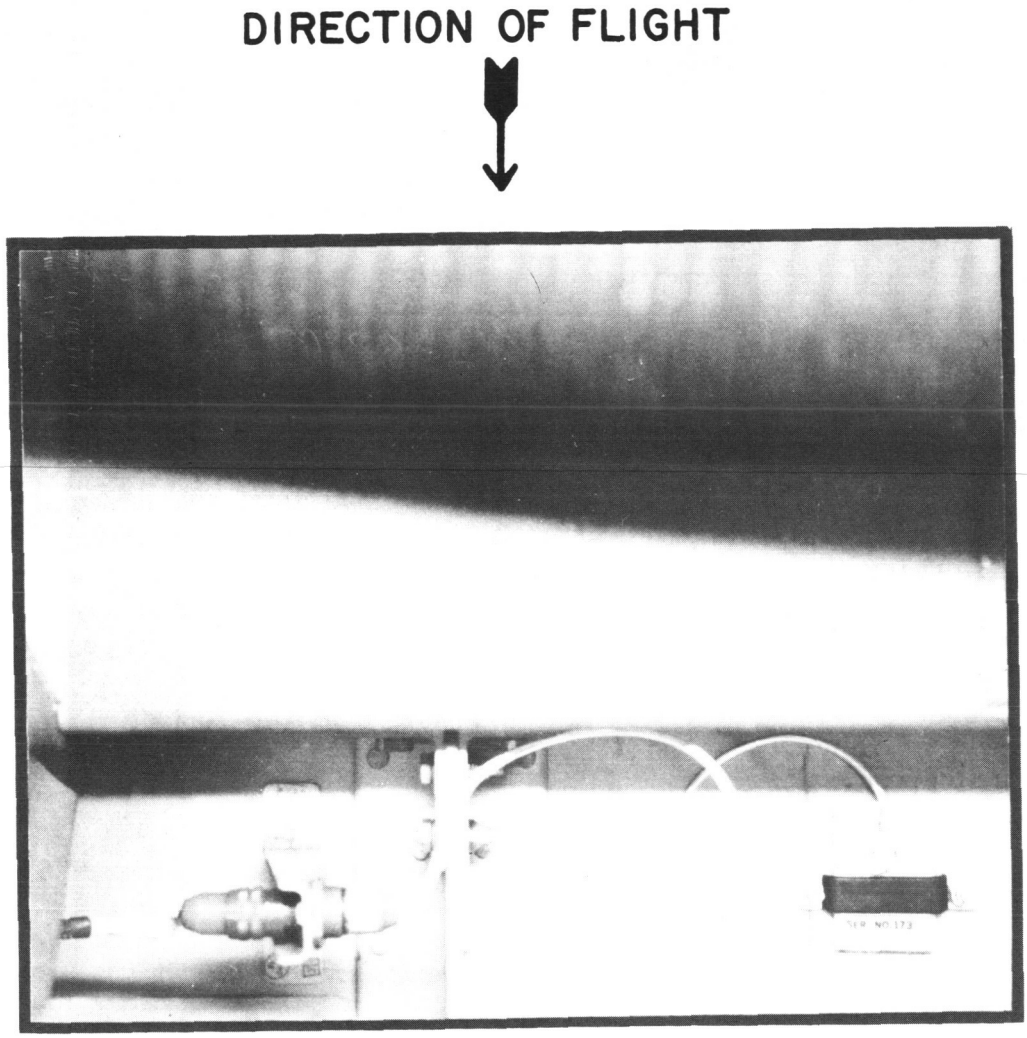

FIGURE 1. A PEGASUS TEMPERATURE PROBE AS SEEN FROM WITHIN THE SERVICE MODULE ADAPTOR

The transmitted data from Pegasus are received by the NASA Space Tracking and Data Acquisition Network (STADAN) and the Green Mountain Propagation Studies Test Facility. Magnetic tapes containing the PCM data are sent to the STADAN receiving center at Goddard Space Flight Center; after being checked and processed, the tapes are forwarded to the MSFC Computation Laboratory for reduction into engineering units by computer. The converted data are stored on 35-mm microfilm in both tabular and graphical form and sent to the Space Thermodynamics Branch (R-RP-T). The microfilm is then checked, logged, and filed chronologically for rapid access by the data analyst. A reader-printer is used to obtain "hard" copies. An example of PAM data is shown in Figure 2, while Figure 3 is an example of the PCM data. Temperature data will continue to be received and analyzed until the end of the Pegasus mission, as shown in Figure 4.

A quick-look analysis of Pegasus PAM temperature data is accomplished on a daily basis using strip-charts obtained from the satellite tracking stations. This effort was initiated for each Pegasus at the time it achieved orbit. For a period of about three days temperature data were recorded and analyzed for each pass of the spacecraft; thereafter, only one pass per day was recorded. The reasons for this quick-look effort were as follows: 1) When Pegasus I was orbited, Pegasus II was already in the final stages of fabrication. Anomalies detected for Pegasus I, such as failure of a particular area of thermal design, could be verified quickly and could, indirectly, suggest modifications needed for the follow-on Pegasus II. As an example, the unexpected rise in Pegasus I SMA temperatures (see p. 11) above prelaunch estimates could have had serious consequences for Pegasus II requiring immediate changes in the SMA thermal design. However, the quick-look analysis of electronics canister temperatures indicated that the thermal design tolerances were sufficiently broad to absorb this new effect. When Pegasus II was orbited, Pegasus III was already in the final stages of fabrication. The preceding remarks concerning Pegasus I apply identically to Pegasus II. 2) Up-to-date knowledge of the satellite thermal status enables the failure of a critical component to be promptly reported to Satellite Control (COMSAT). Ground commands from COMSAT to the satellite can be used to by-pass or shut-off an improperly functioning instrument. 3) Finally, temperature data must be supplied to branches of Research Projects other than the Space Thermodynamics Branch (R-RP-T) on a daily basis.

The strip-chart temperature data are contained within 20 separate channels, each channel representing a particular temperature measurement of a Pegasus component. The data are recorded on the strip-chart as a voltage percentage, the voltage representing the output of a particular temperature probe. Calibration charts, prepared for each satellite before flight, are

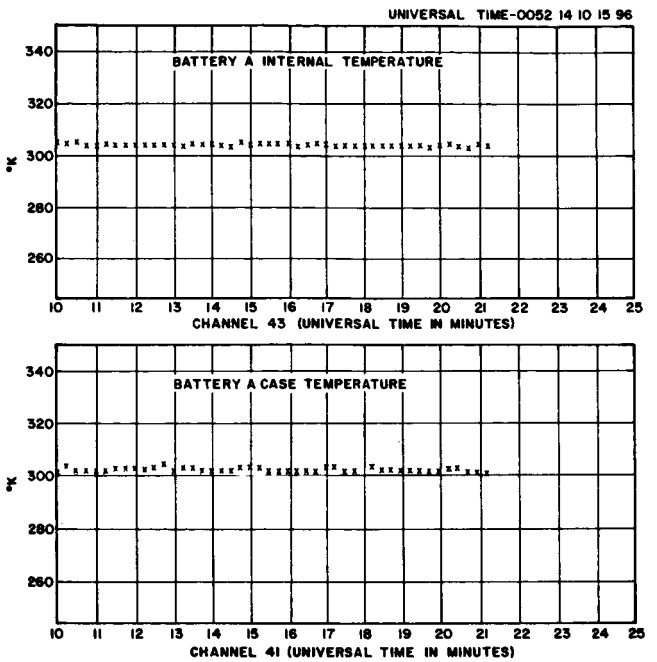

FIGURE 2. PEGASUS I PAM TEMPERATURE DATA

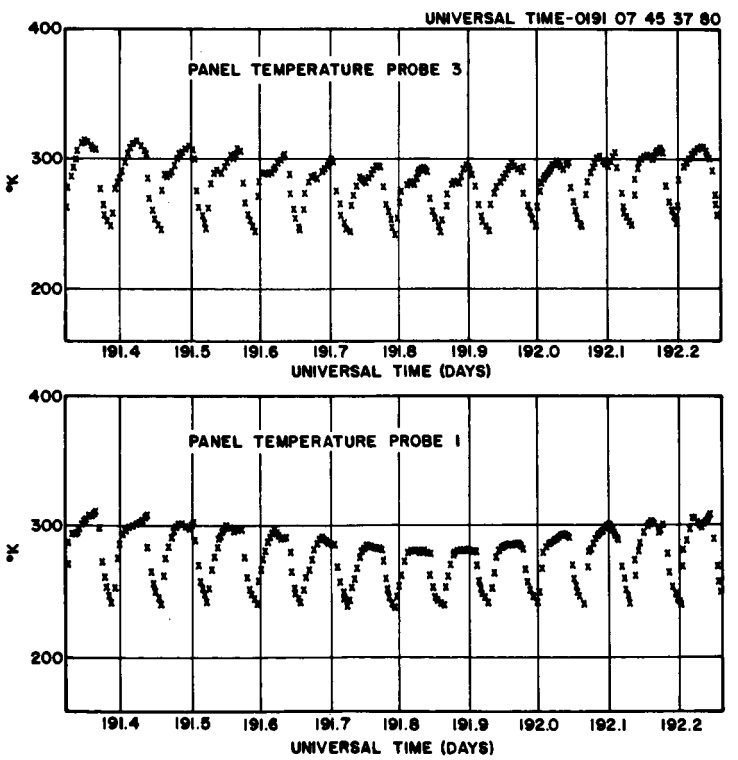

FIGURE 3. PEGASUS I PCM TEMPERATURE DATA

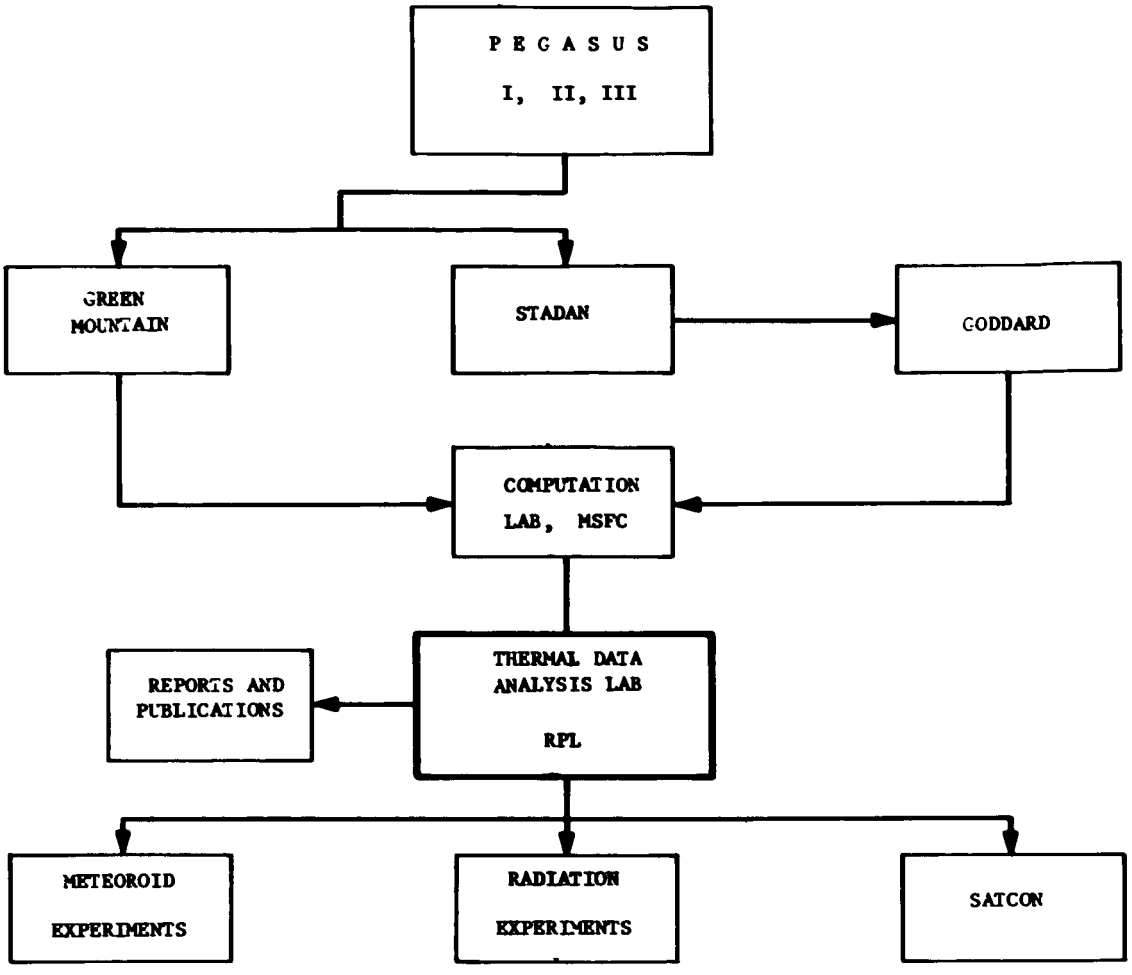

FIGURE 4. FLOW CHART OF PEGASUS THERMAL DATA ANALYSIS

employed to reduce the data to temperature readings. The daily temperature for each channel is plotted as a function of days in orbit. This, then, comprises the source for rapid thermal data access required for the reasons previously mentioned; these graphs also enable the long-term trends to be readily observed for the description of satellite thermal behavior. An example of the quick-look analysis data recorded during the 12-hour interval following launch is shown in Figure 5, while Figure 6 shows the form recorded daily.

The temperature data analysis for Pegasus I, II, and III will continue until the data transmitters are no longer functioning.

SMA COATING DEGRADATION

Thermal Design Summary

Thermal design considerations of the Pegasus electronics canister indicated the need for a large heat sink to absorb the excess radiative energy passing through the louver array, while at the same time shielding the canister from direct solar radiation. As a result, the Pegasus' center structure, containing the electronics canister, was attached to the SMA; the S-IV stage and the instrument unit (IU) of the Saturn vehicle were attached at the base of the SMA for additional heat sink capacity (Fig. 7).

To function as a heat sink, this large area ($\sim$290 m^2) had to be maintained at a low temperature. This is accomplished most easily by minimizing the heat input from the sun and the earth; i.e., by coating the exterior surface with a substance with a low solar absorptance (α_s) and high infrared emittance (ϵ_{IR}). Determination of orbital skin temperatures as a function of α_s/ϵ_{IR} was obtained by bracketing the expected orbital conditions for the Pegasus satellite [1] and by using the General Space Thermal Program with the IBM 7090 computer. The allowable range of α/ϵ for canister thermal stability was confined to $0.2 \leq \alpha/\epsilon \geq 0.3$ for the most extreme (hottest) orbital conditions (e.g., 78 percent time in sunlight).

Upon the recommendation of E. R. Miller, R-RP-T, MSFC, a methyl silicone paint pigmented with ZnO* (S-13) was selected as the thermal coating for the SMA, IU, and S-IV stage. For the S-13 coating, $\alpha_s/\epsilon_{IR} = 0.22$. Laboratory tests to determine radiometric property stability were performed on S-13 samples at the IIT Research Institute (IITRI); after 200 hours exposure to

* S-13 was developed under contract by IITRI.

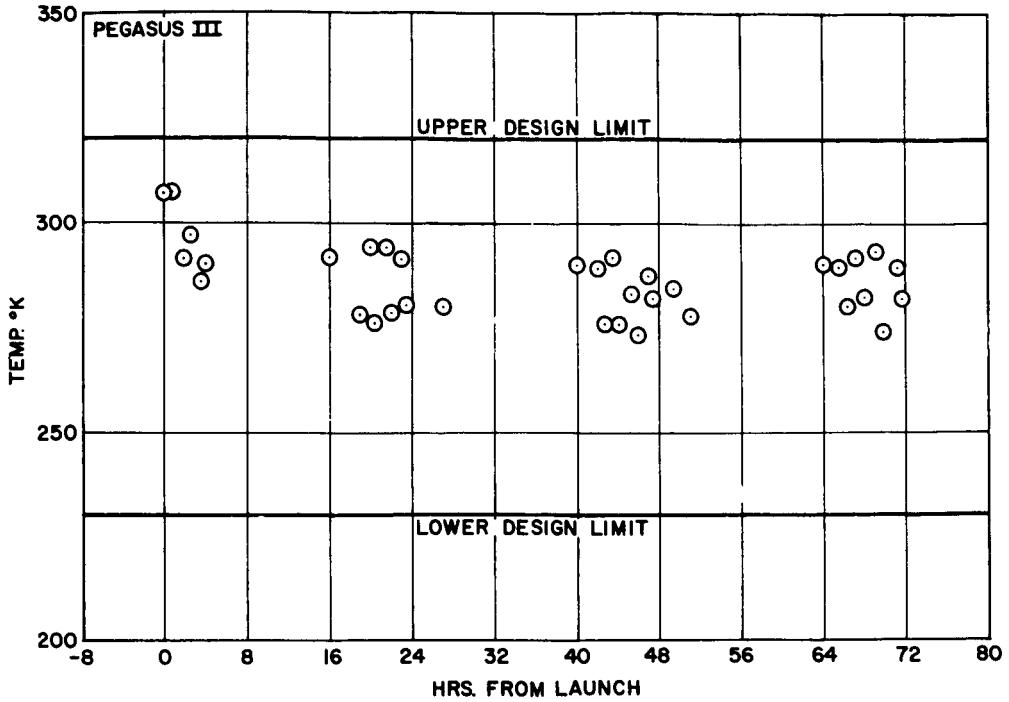

FIGURE 5. EARLY POST-LAUNCH TEMPERATURE COVERAGE-RADIATION DETECTOR

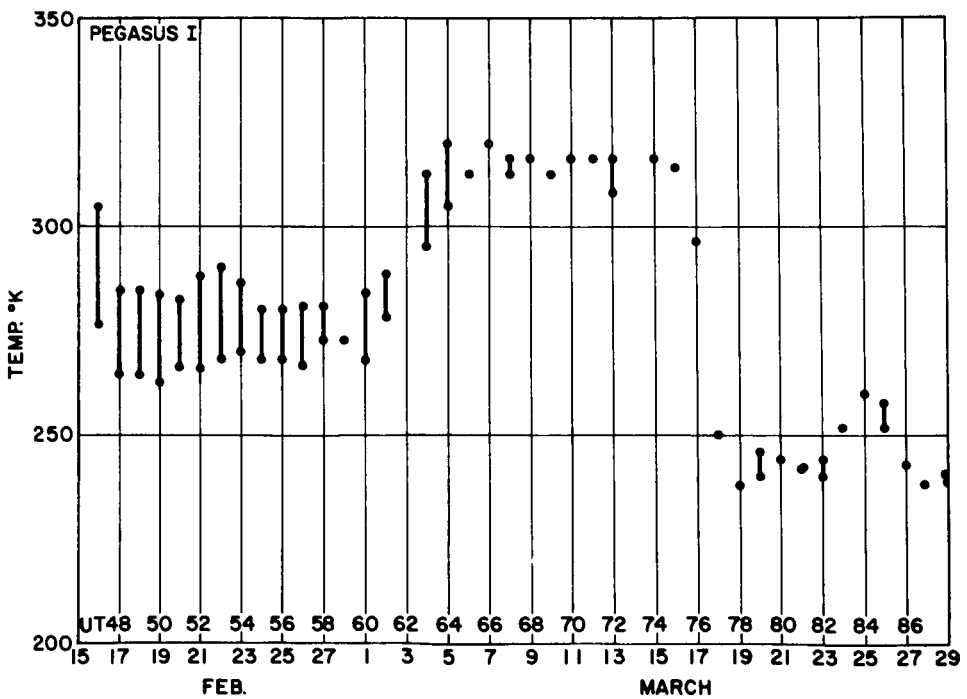

FIGURE 6. TYPICAL DAILY TEMPERATURE COVERAGE-CHANNEL 36-RADIATION DETECTOR

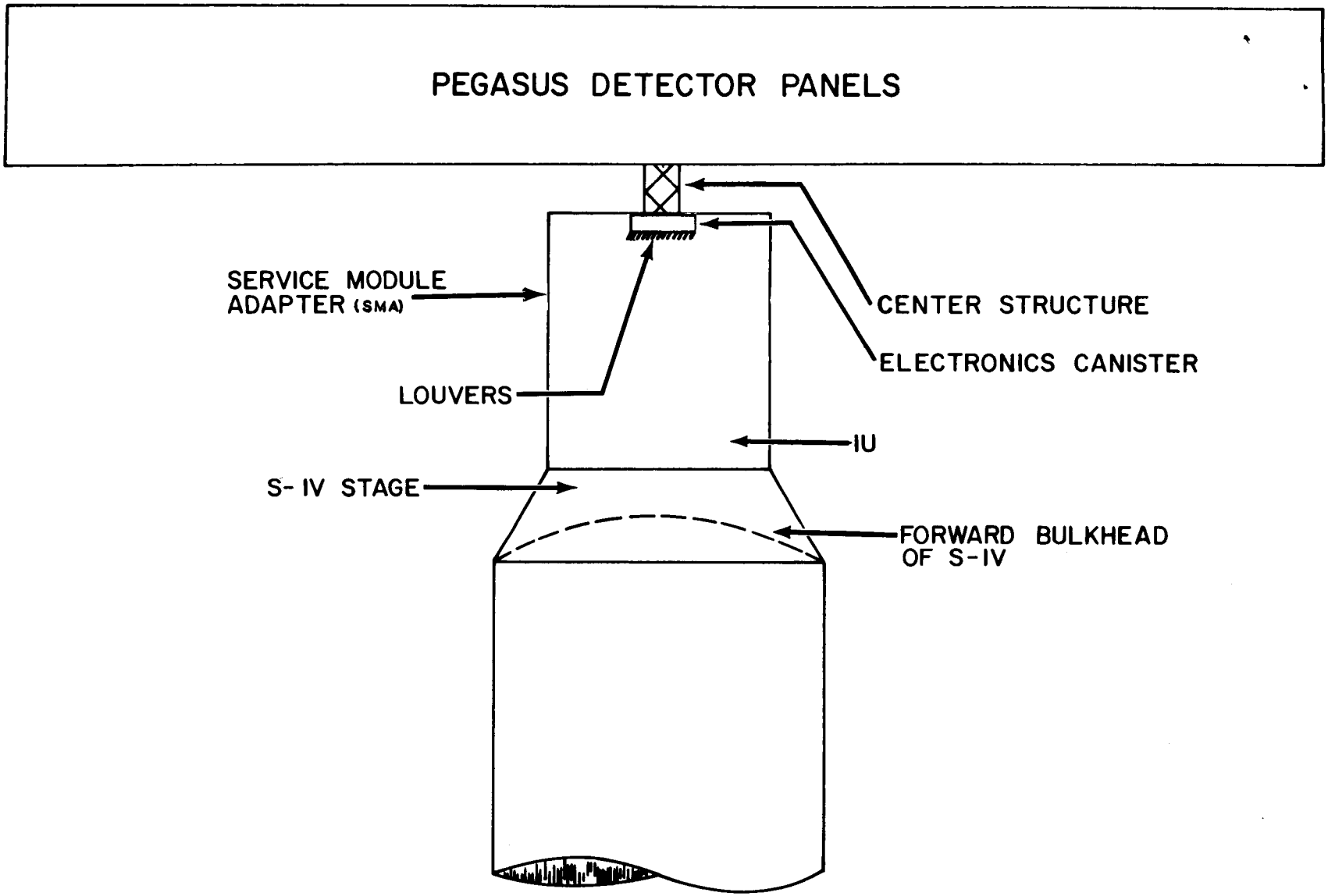

FIGURE 7. OPEN END OF THE SATURN VEHICLE AS A TEMPERATURE SINK

ultraviolet radiation (10 "suns" intensity) the change in the absorptivity of the S-13 coating was only +0.04.

Prelaunch, on-the-pad measurements of the α/ϵ ratio made by Research Projects Laboratory (MSFC) and Fairchild-Hiller personnel, using newly developed portable reflectometers and emissometers, indicated a value of 0.21 for the SMA and 0.24 for the S-IV stage. Particular care was taken in detecting (and preventing) any visible surface degradation while the vehicles were prepared for launch, including a thorough and carefully administered washing shortly before launch.

On February 13, May 25, and July 30, 1965, the three Pegasus satellites were placed in their respective orbits. In each case, postlaunch quick-look comparison of SMA temperature data indicated an α/ϵ ratio of approximately double the prelaunch value (Table I and Fig. 8).

Temperatures monitored from the SMA never fell within the expected (prelaunch) range. Surface degradation sufficient to cause this α/ϵ ratio increase was, indeed, of a serious and consequential magnitude. The methods employed in defining this degradation quantitatively are described, and a discussion of the cause follows.

Procedure *

Three temperature probes were located circumferentially at the base of the SMA at 120° intervals to monitor the orbital temperatures. Voltages proportional to temperature were relayed to ground station by PAM telemetry, and the subsequent data were reduced by personnel of R-RP-T to arrive at an average daily temperature for the SMA. Temperature probes within the S-IV stage were not instrumented to function after engine shutdown; S-IV temperatures, as a result, are not accessible for thermal analysis. This precludes the possibility of determining the longitudinal variation of α/ϵ (along the X-axis); however, it is the gross degradation of the S-13 coated surface that is of primary concern, and this was determined as follows.

* The procedure and results outlined in this section apply only to Pegasus I. The complex motion of Pegasus II and III has hampered their thermal analysis to the extent that, at present, only qualitative generalizations are applicable.

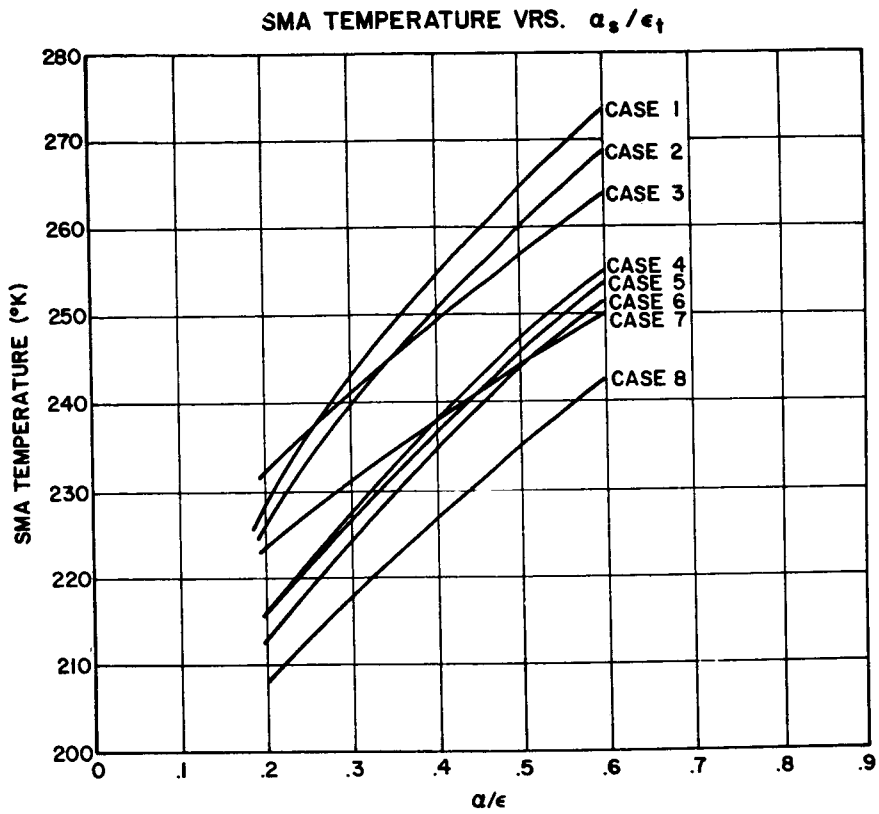

The Different Cases Refer to Various Orbital Conditions. Case 5 Represents a Typical Day in Orbit. Considering the Average SMA Temperature (T≅250), Case 5 Shows $\alpha/\epsilon = .55$.

CASE 1
$T_X = .78$
$F_{\gamma r} = .5$
cos(MAS) = 1
no flux through open end

CASE 2
$T_X = .78$
$F_{\gamma r} = .5$
cos(MAS) = 1
$\alpha_2 = \epsilon_2 = 0.9$

CASE 3
$T_X = .78$
$F_{\gamma r} = .5$
cos(MAS) = .637
$\alpha_2 = \epsilon_2 = 0.9$

CASE 4
$T_X = .78$
$F_{\gamma r} = .5$
cos(MAS) = .637
no flux through open end

CASE 5
$T_X = .63$
$F_{\gamma r} = .25$
cos(MAS) = 1
$\alpha_2 = \epsilon_2 = .9$

CASE 6
$T_X = .63$
$F_{\gamma r} = .25$
cos(MAS) = 1
no flux through open end

CASE 7
$T_X = .63$
$F_{\gamma r} = .25$
cos(MAS) = .637
$\alpha_2 = \epsilon_2 = .9$

CASE 8
$T_X = .63$
$F_{\gamma r} = .25$
cos(MAS) = .637
no flux through open end

FIGURE 8. PRE-LAUNCH CALCULATIONS FOR PEGASUS I

The basic calorimetric equation used in this analysis (Appendix) was modified to a form compatible with the average SMA temperatures available as input. This was accomplished by integrating the equation over time. As a result of this integration, the conduction, radiation, and $\dot{T}_i$ terms vanish. Since the internal heat generated by the electronics is so small compared to the heat sink volume, $\dot{Q}_i$ is also effectively zero. Thus, we have the integrated equation

$$0 = A_{1i}\,\alpha_i\,S + A_{2i}\,\alpha_i\,BS + A_{3i}\,\alpha_i\,ES - A_{4i}\,\epsilon_i\,\sigma\left(\frac{T_i}{100}\right)^4 .$$

There were three areas of consideration:

1. The surface area of the SMA, IU, and S-IV stage ($A_{4i} = 288.5\ m^2$)
2. The open end of the SMA ($A_{42} = 11.3\ m^2$)
3. The nozzle end of the S-IV stage ($A_{43} = 23.6\ m^2$)

The nozzle end of the S-IV stage could only be considered in an approximate manner, as no temperature sensors were located at the base of the S-IV stage; the effect of this area on the overall thermal situation was not accessible to precise analysis. This approximation is discussed in more detail later in this report.

Pegasus I, after initial orbiting, very quickly opened its half cone angle of spin about the longitudinal X-axis to 90° such that it moved in a flat tumble in a slowly varying plane. For the cylindrical walls of the SMA, IU, and S-IV stage, an appropriate tumbling factor [3] was included in the effective area to solar radiation (A_{11}). For the open end of the SMA, the effect of the flat tumble was compensated for by considering the "flat plate" effective areas to be cylindrical.

Finally, upon substitution for the effective areas, we have (for Pegasus I only):

$$\alpha_1/\epsilon_1 = \frac{\left[A_{41} + A_{42}\right]\sigma\left(\frac{T}{100}\right)^4 - ES\left[\frac{A_{41} F_{\gamma_1 r}}{\pi} + \frac{A_{42} F_{\gamma_2 r}}{\pi}\right] - \frac{SA_{42}}{\pi}\left[T_x \sin MAS + BF_{\gamma_2 r}\,\overline{\cos RAS}\right]}{\frac{A_{41}S}{\pi}\left[\Gamma_x \rho + BF_{\gamma_1 r}\,\overline{\cos RAS}\right]},$$

where ρ is the tumbling factor. (The open end of the SMA (A_{42}) was assumed to approximate a grey body radiator with $\alpha_2 = \epsilon_2 = 0.85$.)

Some of the input parameters included in the above equation were obtained by an averaging process. For example, the geometry factors $F_{\gamma_1 r}$ and $F_{\gamma_2 r}$ were assigned an average value of 0.85, obtained from curves of F versus satellite altitude [4]. The term $\overline{\cos RAS}$ was obtained from the equation

$$\overline{\cos RAS} = \frac{\cos \delta}{\pi}$$

a derivation originating from the observation that absorbed albedo is zero for that part of an orbit when the satellite is in the earth's shadow. The grey body approximation for A_{42} was suggested by physical reasoning. The remaining input paremters were obtained from computed and telemetered attitude data.

An error analysis was conducted to determine the effect these approximations would have on the final results, using a standard formula for probable error. The variance of the individual parameters under study was determined, most often, by inspection of appropriate graphs. The probable error determined by this method is approximately 10 percent.

Results

Following the derivation of the basic equations to be used, the literature was scanned for available input data [3,4]. The data were organized, and the resulting values of α/ϵ were obtained (Fig. 9). An interesting implication of these results concerns the relatively small S-13 degradation after the initial rise of the α/ϵ ratio.

It should be mentioned at this point that about 30 percent of the solar absorptance increase for S-13 observed on Pegasus I, II, and III can be explained by the "in situ" phenomenon; this is a descriptive term used to describe a recently discovered [5] anomalous "bleaching" of thermal control coatings in air after removal from an in-vacuo ultraviolet irradiation test facility. For

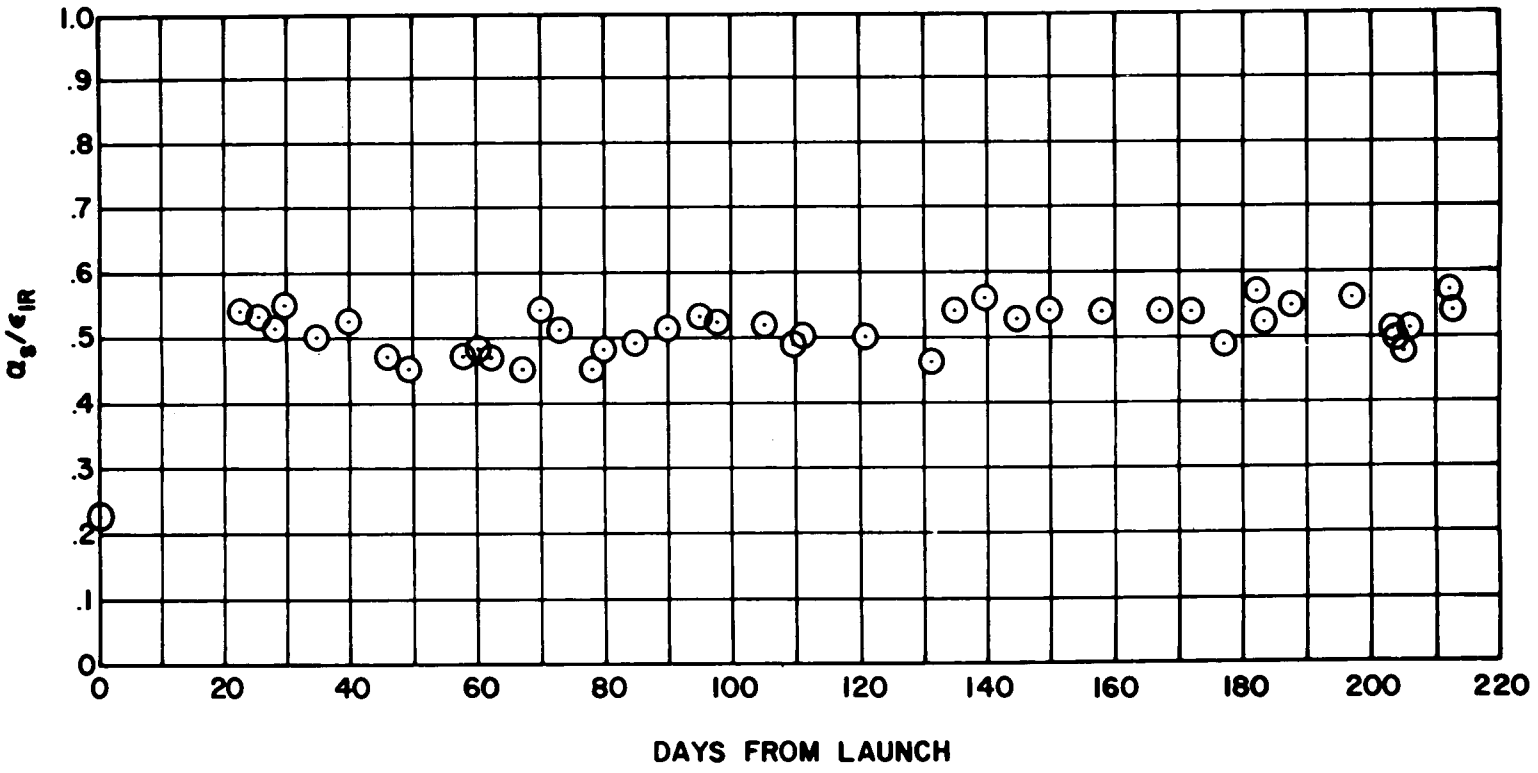

FIGURE 9. S-13 COATING DEGRADATION ON THE PEGASUS I SMA

example, in a vacuum, under UV irradiation, the solar absorptance of a sample of S-13 will increase approximately 30 percent; when the sample is removed from the vacuum chamber and the reflectance measured in air, the sample is seen to have "bleached" and littile, if any, degradation is observed (Fig. 10). Thus, from laboratory results, it can be stated that 30 percent of the increase in the S-13 solar absorption observed on the three Pegasus satellites can be accounted for by the "in situ" effect. The remaining 70 percent increase is unexpected for an S-13 surface in space and requires some other explanation.

Calculations prior to March 8, 1965, are lacking because of the motion of Pegasus I in this period. The satellite was initially spinning only about its X-axis, although, since the Z-axis lies along its principal moment of inertia, a precessional motion about the X-axis was soon established (Fig. 11). The half cone angle steadily opened to the full $\pi/2$ radians, at which time the satellite was in a flat tumble about the Z-axis and temperature analysis was possible.

The motion of Pegasus after the time represented by the latest α/ϵ value shown in Figure 9 degenerated from the stable tumble characteristic of the initial months in orbit. The principal momentum vector of the satellite, oriented along the Z-axis, began oscillating more rapidly with respect to the sun vector. The angle MAS, characteristic of this motion, is illustrated for comparison in Figure 13; the more rapidly varying angle MAS results in a more rapidly varying SMA temperature and, thus, decreases the accuracy of the calculations. Values of the SMA α/ϵ ratio determined through the first half of 1966, although widely scattered, show a discernable consistency which indicates, approximately, a 20 percent increase above the early post-launch values.

A plot of α/ϵ as a function of the angle MAS was also generated (Fig. 12). The directional dependence indicated by this curve was not observed in pre-launch radiometric measurements, nor was it expected. The explanation may involve surface damage resulting from LOX diffusion through the skin of the S-IV stage.

The most plausible explanation for the increased solar absorptance involved contamination.* It has been shown that ultraviolet irradiation of a contaminated S-13 coated surface results in significant degradation. A consideration of the possible sources of contamination to the SMA and S-IV surfaces leads to the conclusion that the S-IV stage retro-rockets, which fire at booster engine cutoff , are the most probable source. However, detailed examination

* The emittance of S-13 is assumed constant; this assumption is based on a consideration of the physical process necessary for a decrease emittance.

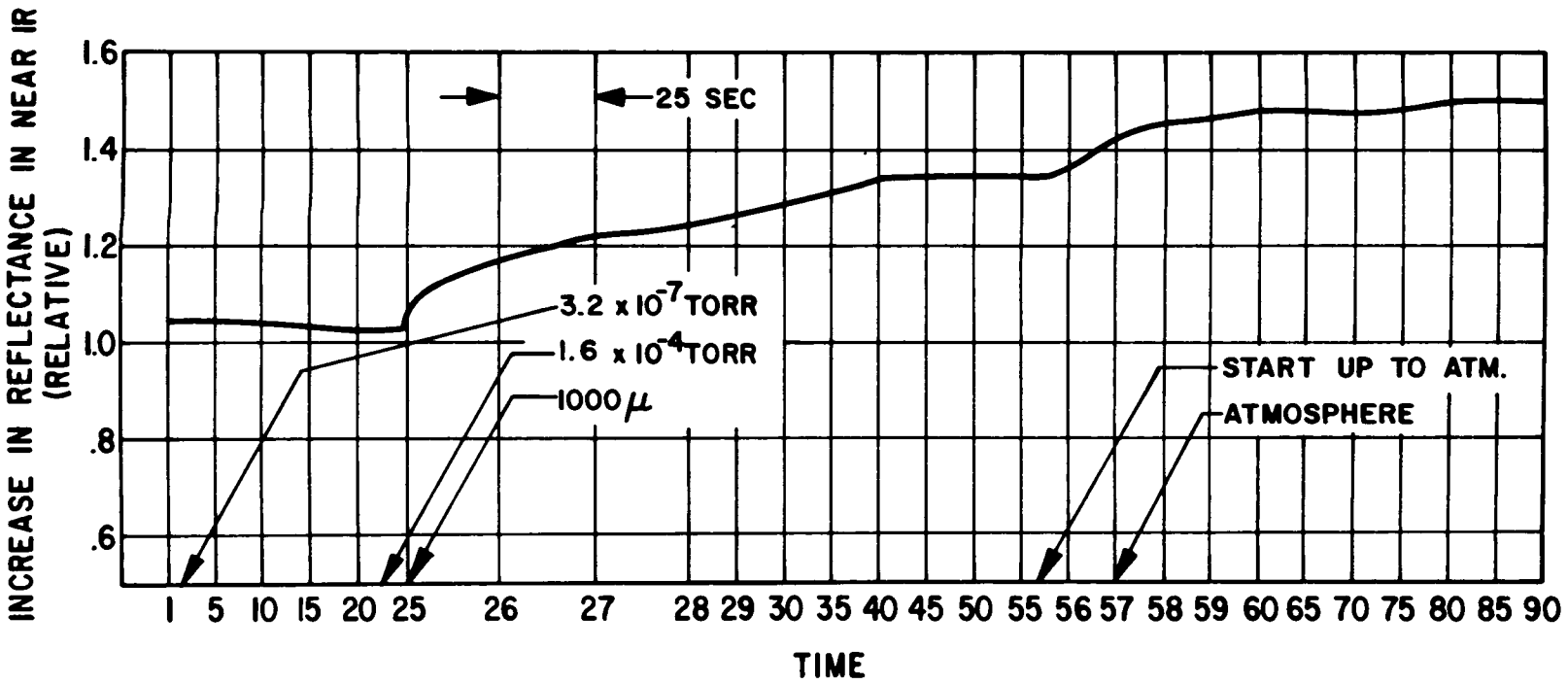

FIGURE 10. EFFECT OF ATMOSPHERIC EXPOSURE TO UV DEGRADED S-13

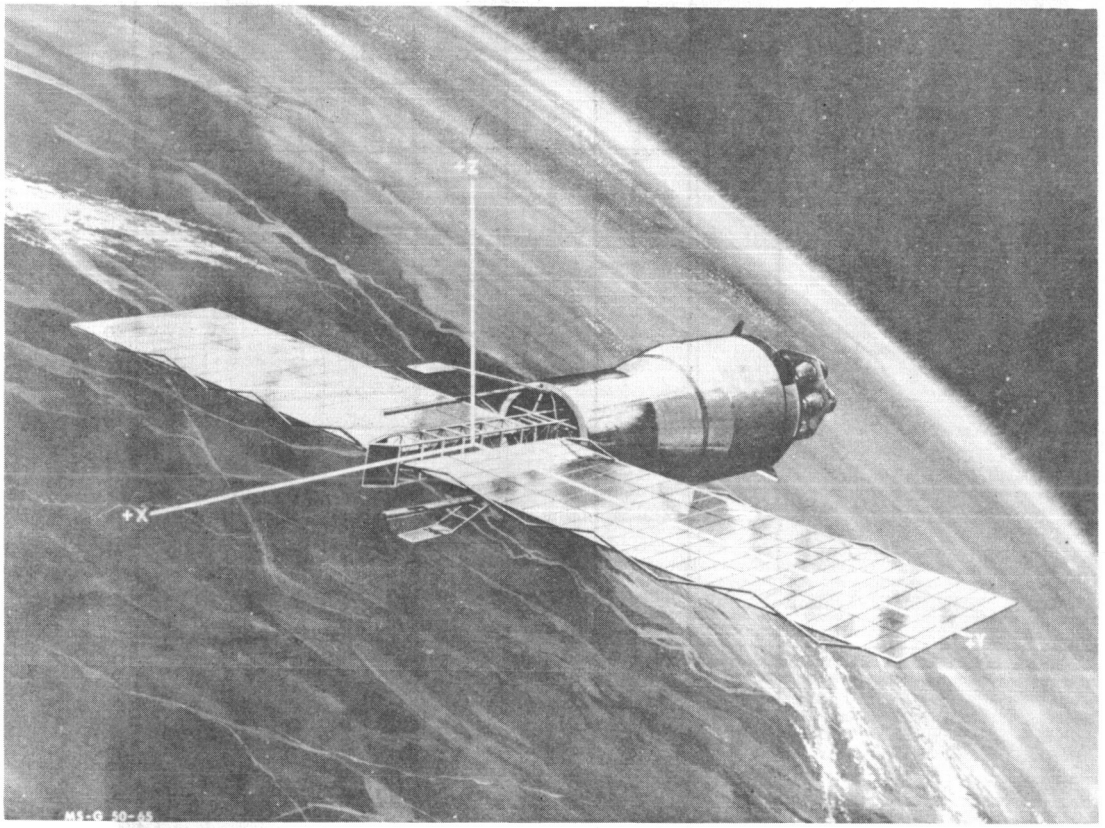

FIGURE 11. PEGASUS SATELLITE SHOWING ORIENTATION OF AXES

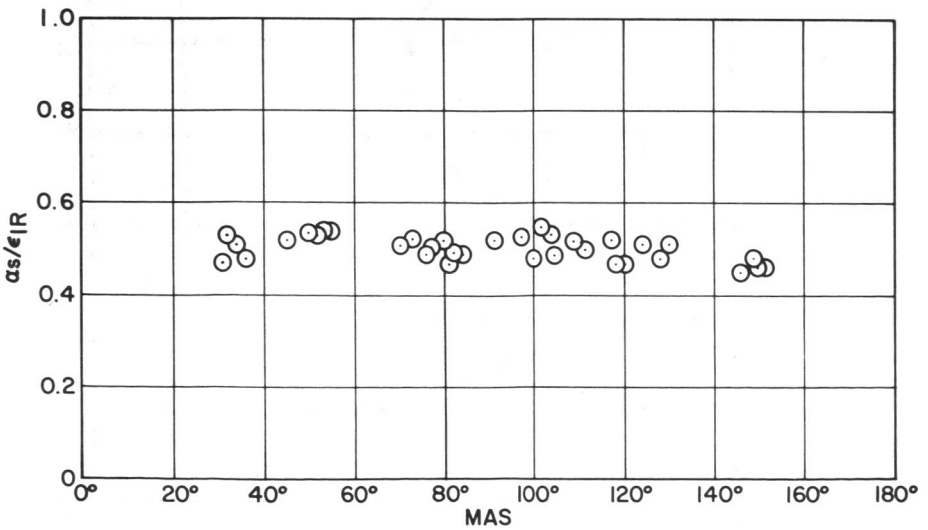

FIGURE 12. SMA DEGRADATION AS A FUNCTION OF SUN ASPECT ANGLE (MAS)

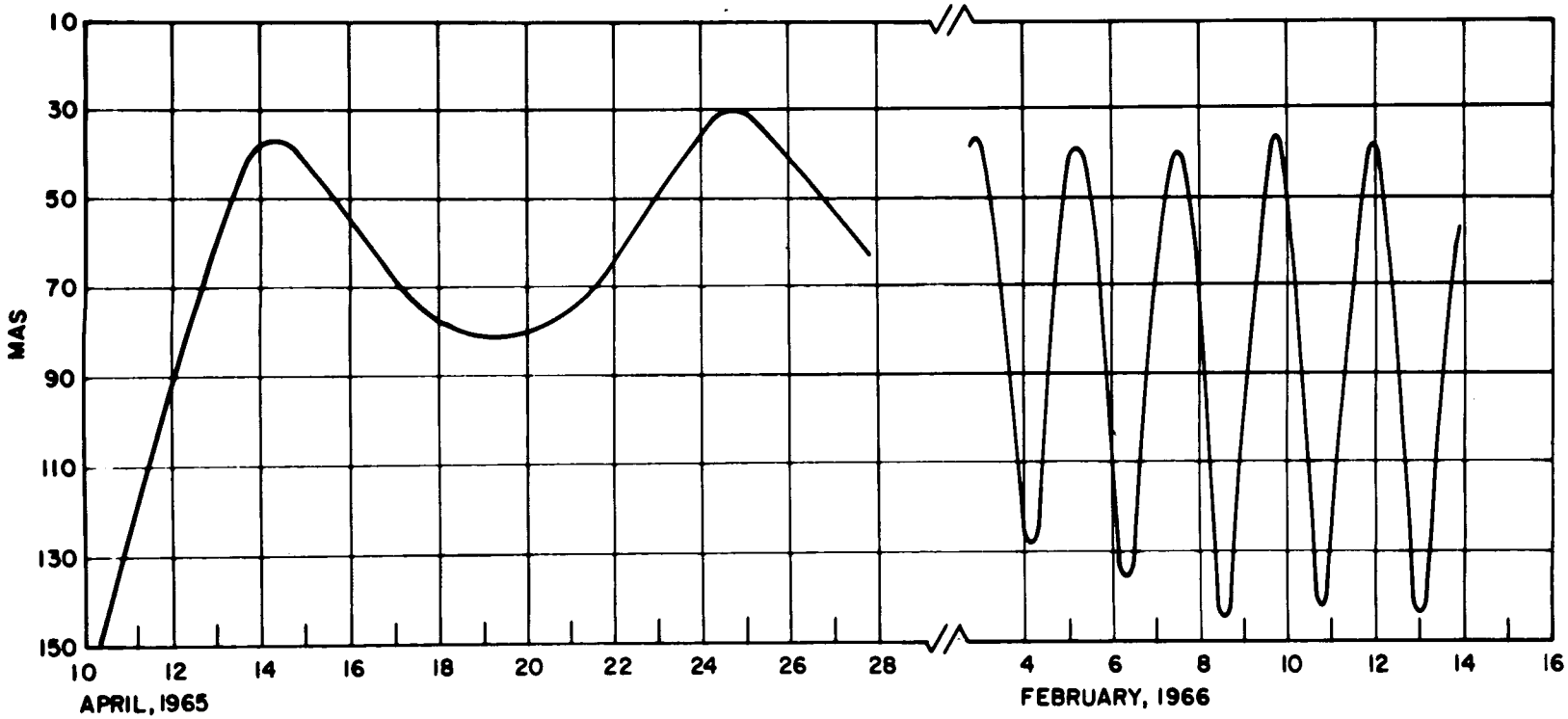

FIGURE 13. MAS ANGLE SHOWING OSCILLATION OF PRINCIPAL MOMENTUM VECTOR

of 35 and 70-mm films covering the launch of SA-9 with Pegasus I, particularly the frames showing retro-rocket firing, has added little support to this theory. It is very reasonable to expect that contamination of sufficient extent to double the magnitude of the solar absorptance would most certainly be visible; the darkening would be considerable. Although the films examined do not contain the optimum viewing capability--the S-IV stage retro-rockets were fired at an altitude of approximately 90 km--it is curious that no shadowing of the S-13 surface is detectable. As a result, plume impingement as a cause of the degradation is still only speculation.

In an effort to determine what effect retro-rocket firing does have on S-13, a retro-rocket was fired in the Arnold Engineering Development Center (AEDC) J-2 facility, which nominally simulated altitudes of about 40 km, with samples of S-13 placed in positions analogous to the side of the S-IV stage. During the test on November 11, 1965, the reference panel hidden from direct plume impingement showed very little degradation, while all the samples impinged by the plume showed considerable loss in reflectance. Whether or not this actually isolates the source of contamination to the S-13 surfaces on SA-9 depends upon the degree of similarity of the AEDC J-2 facility to the conditions of SA-9 at retro-rocket firing time. As yet, only altitude and vacuum conditions have been shown to be similar.

The venting rate of the excess fuel from the S-IV stage, after orbital insertion, is a function of the temperature of the S-13 coated skin of the S-IV stage. The hotter temperatures resulting from an increased solar absorptance would, therefore, increase the venting rate of the vaporized liquid hydrogen fuel, which, except for certain associated parameters, should be a readily apparent indication of S-13 degradation caused by retro-rocket plume impingement. Aside from skin temperature, the controlling factor of hydrogen venting rate is the quantity of liquid H_2 left in the fuel tank. Data were obtained that predicted venting thrust for three levels of residual LH_2 . Data from SA-9, including LH_2 tank pressures and temperatures, were analyzed to define the discrepancy between prelaunch estimates and postlaunch performance of venting rates. Unfortunately, the data are insufficient for the task and as yet no conclusion is possible.

When orbital temperatures are (as in this case) about 40° K higher than expected, the question naturally arises as to the accuracy of the temperature probe readings. (The accuracy of theoretical calculations can be seen by studying part III of this report). However, three consecutive Pegasus launchings have resulted in nearly identical SMA temperatures, which lessens the uncertainty. It has been suggested that direct sunlight is impinging on the probes; however, the

interior geometry of the SMA tends to dispel this speculation, considering the "hidden" location of the probes. It should also be mentioned that all three probes read higher at the same time, an unlikely state of affairs if the latter phenomenon should occur.

Although the effect of the nozzle end of the S-IV stage on the thermal calculations is not accessible to precise analysis, its effect on the residual hydrogen gas, unvented from the fuel tanks of the S-IV stage, is of prime importance. The total conductance through the low-pressure gas is very high; the heating effect resulting from such conduction could account for the increased temperature readings of the SMA sensors. Unfortunately, no instrument is on board Pegasus' S-IV stage to record fuel tank pressure or temperature after initial venting. One can only speculate that sufficient gas was left in the tanks to conduct an ample quantity of heat to the SMA and raise the average temperature. "Worst case" calculations of this effect are incomplete and will be reported at a future date.

In conclusion, it should be mentioned that the most positive indication of plume impingement causing S-13 degradation is the result of a study of the space environmental effects sensors flown as a supplementary experiment aboard Pegasus. One of the thermal sensors included in this package was protected from plume impingement by the SMA shroud during ascent; it has been found that the S-13 coating on this sensor did not undergo degradation greater than five percent. This suggests, to some extent, that protection from plume impingement will prevent degradation; thus, indirectly pointing to the cause of the S-13 degradation on the SMA.

The complicated attitude of Pegasus II and III has hampered the thermal design evaluation. However, a comparison of SMA temperatures, averaged over a long period of time for each of the three vehicles, leads to the conclusion that the remarks made for Pegasus I are directly applicable to Pegasus II and III (Fig. 14). All three have undergone the same 50-percent increase in the α/ϵ ratio for the S-13 coating, and the coating stability is apparently very similar. All three spacecraft, despite this phenomenon, have temperatures well within the tolerance of the prelaunch thermal design.

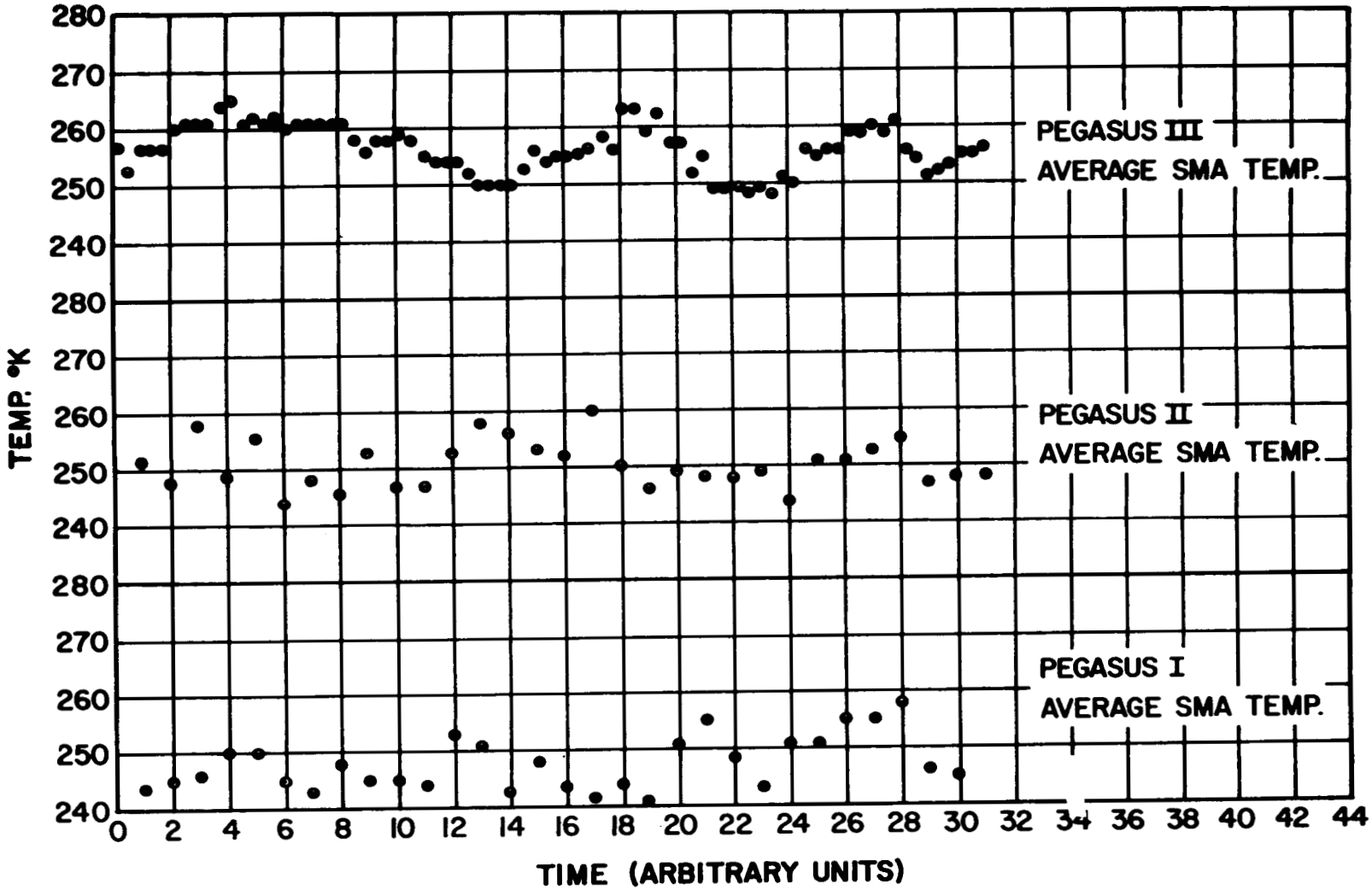

FIGURE 14. COMPARISON OF LONG-TERM AVERAGED SMA TEMPERATURES. THE TIME SCALE COVERS APPROXIMATELY NINE MONTHS

LOUVER SYSTEM PERFORMANCE

Thermal Design Summary

The essential electronics instrumentation for the Pegasus spacecraft was enclosed in an insulated canister located in the lower portion of the center structure (Figs. 15 and 16). A significant proportion of the power input to the various components of this "electronics canister" is dissipated as heat energy. Since the power input is a function of solar cell array attitude, the thermal output is a varying parameter. As a result, the thermal design of the electronics canister was approached by bracketing the expected thermal fluctuations about the design tolerances of the more sensitive components. Thermal linkage between components and supporting structures was minimized, and superinsulation "blankets" (highly reflective sheets of aluminized Mylar) were placed around the canister walls. A "sized" window was originally envisioned for the bottom of the canister to radiate excess heat to the SMA sink; however, calculations of expected canister performance indicated the insufficiency of completely passive thermal control [1]. An active thermal control system was required (and built) employing a lightweight set of active louvers controlled by a bimetallic actuator (Fig. 17). The set of louver blades was designed such that each blade is independently actuated. The adequacy of this design was demonstrated in a series of in-vacuo tests.

The only serious problem that arose in the design of the louver system involved the thermal insulation of the actuator. Originally, it had been designed so that the actuator responded only to the canister temperature fluctuations, remaining unaffected by the thermal state of the SMA sink. To accomplish this, the actuator was insulated to allow only radiative linkage to the canister. In tests, however, the actuator continued to respond to SMA thermal fluctuations. It was found that the situation could be remedied, to some degree, simply by changing the actuation temperature. As a result, postlaunch calculations of louver blade opening angle versus louver temperature were performed by calculating a radiometric mean louver temperature between canister and SMA temperature and assuming the louver blade and actuator were at the same temperature. In an attempt to determine the error introduced in the computations by this assumption, a study done at Fairchild-Hiller Corporation* was used as a guide.

* Fairchild-Hiller Corporation was the prime contractor for the Pegasus spacecraft.

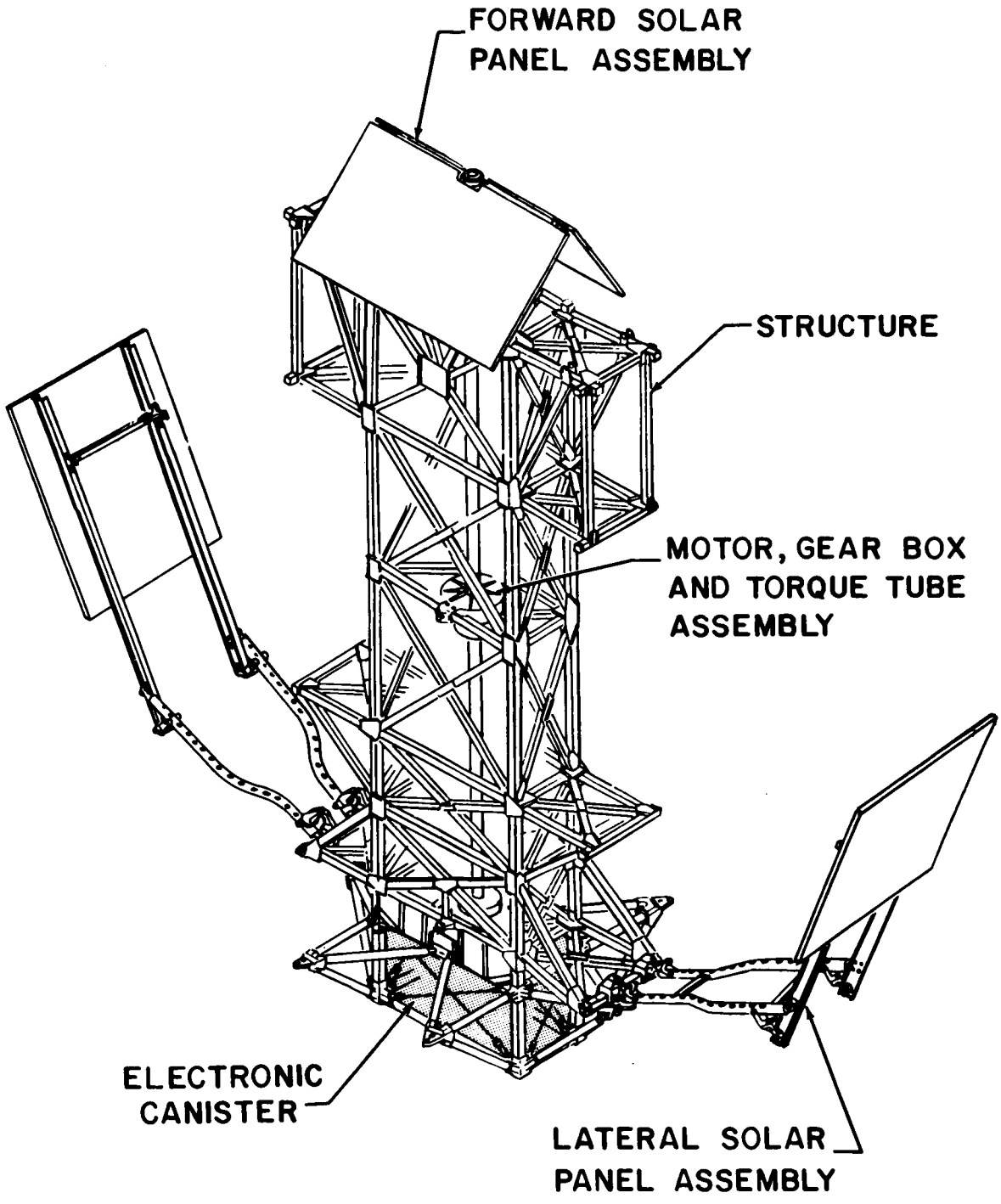

FIGURE 15. CENTER SECTION

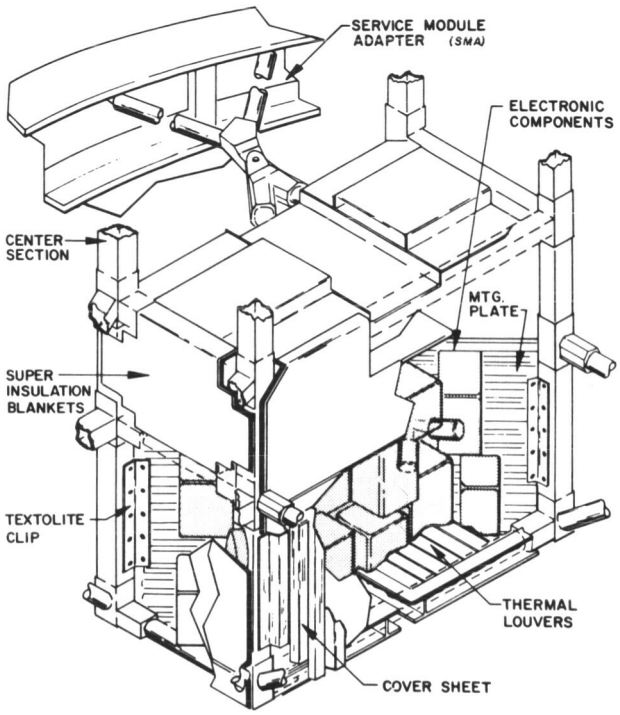

FIGURE 16. ELECTRONICS CANISTER

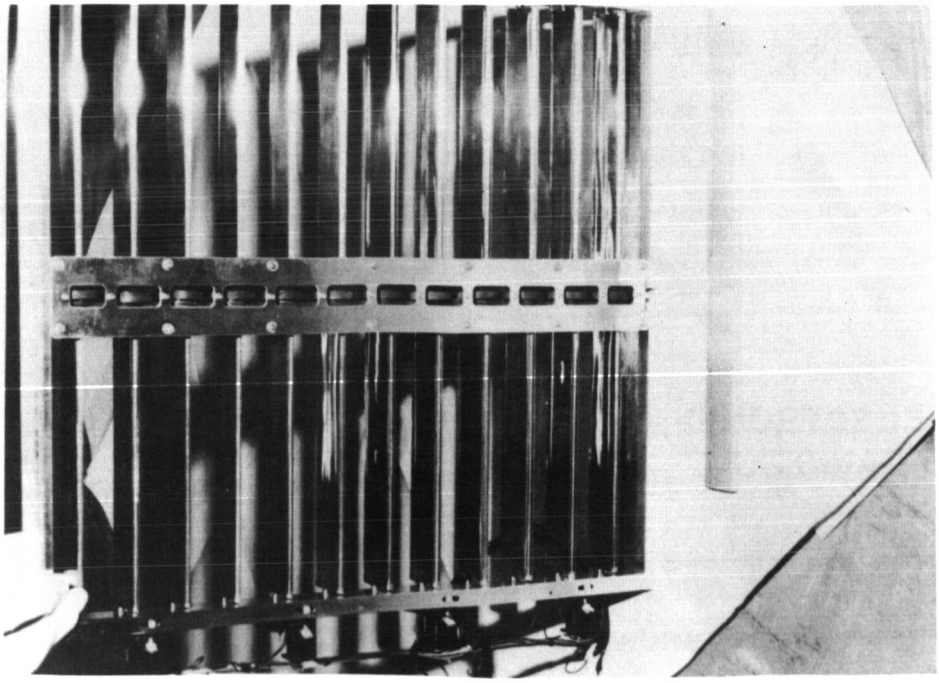

FIGURE 17. THERMAL CONTROL LOUVERS

A determination of actuator temperatures as a function of the component and radiation sink temperatures was made for a series of hot and cold cases in a vacuum chamber. The discrepancy between these curves and a calculated radiometric mean was obtained for the louvers in both the open and closed position. By inspection of a set of calibration curves of blade angle versus temperature, the difference in louver blade opening angle for the two actuator temperatures was then obtained, considering the inherent leeway allowable in louver blade opening angle as a control on the canister temperature. The difference in blade angle ($\theta = \pm 8°$) determined by the two methods is considered to be negligible.

Procedure and Results

The essential tasks in the thermal design evaluation of the Pegasus louver system were to verify operation in orbit and to describe the performance over an extended period of time. The first of these objectives was accomplished with the aid of the following equation [1]:

$$AF\,\sigma\left[\left(\frac{T_s}{100}\right)^4 - \left(\frac{T_c}{100}\right)^4\right] + \dot{Q}_i + \dot{Q}_g = 0 \quad ,$$

where

A = area of louver system

F = effective emissivity

$\dot{Q}_i$ = extraneous heat loss through insulation, etc.

$\dot{Q}_g$ = average orbital internal heat generation of the canister

σ = Stefan-Boltzmann constant (5.67 joule/deg^4 - m^2 - sec)

T_s = temperature of SMA "sink"

T_i = average internal temperature of canister

A detailed examination of the electronics canister thermal output (the I^2R loss) was initiated with the objective of determining the range of $\dot{Q}_i$. Final values chosen, corresponding to "hot" (maximum T_x) and "cold" (minimum T_x) cases, were 35 W and 15 W, respectively. Numerical values of $\dot{Q}_g$ are selected from the results of an in-vacuo test of the louver system in conjunction with a simulated electronics canister. As for the generated heat, $\dot{Q}_i$, extreme values of $\dot{Q}_g$ were

chosen for a "hot" and "cold" case. A linear curve was drawn through these points enabling, for a given T_x, the selection of the corresponding value of $\dot{Q}_g$. The temperatures T_s and T_c were obtained by an averaging process using telemetered PAM temperature data.

Considering a "hot" and "cold" case (determined from graphs of T_x as a function of days from launch), the above equation was solved for F, the emissivity factor. These values of F were compared to a theoretically derived curve of F versus louver blade opening angle [6] to determine the blade angle necessary for a given set of input data. This procedure was followed for each of the three Pegasus utilizing the appropriate prelaunch and orbital data for each. The results indicate the louver systems are working successfully* on each of the three satellites (Tab. I).

The second objective, describing louver system performance over an extended period of time, was accomplished assuming the louver temperatures to be

$$T_L^4 = \frac{T_s^4 + T_c^4}{2} ,$$

where

T_L = louver temperature

T_s = SMA sink temperature

T_c = canister temperature (mean)

(See page 20 for a discussion of this assumption.)

The temperatures T_c and T_s were obtained by an averaging process from telemetered Pegasus temperature data. Comparison of the resulting T_L with prelaunch calibration curves yielded the corresponding louver blade angle for a particular day in orbit. This procedure was duplicated many times for each Pegasus satellite; the resulting louver blade opening angles, obtained as a function of both T_x and days launch, were plotted in a series of graphs that serve to give an informative description of the Pegasus louver systems in operation (Figs. 18, 19, and 20).

The results of the successful operation of the louvers are indicated in Table II. These results are especially satisfying when the higher-than-expected SMA temperatures are considered. A more descriptive portrayal, considering the design limits, is shown in Figures 21, 22, and 23. The battery temperatures are representative of the other canister electronics.

* "successful operation" as used in this instance, means the louvers are open in the "hot" case and closed in the "cold" case.

TABLE I. HEAT BALANCE ANALYSIS OF PEGASUS LOUVERS

PEGASUS I

"Cold" Case (Feb. 20, 1965)	"Hot" Case (June 13, 1965)
$\left(\frac{T_s}{100}\right)^4 = 38.24$	$\left(\frac{T_s}{100}\right)^4 = 42.62$
$\dot{Q}_g = 44$ W	$\dot{Q}_g = 58.5$ W
$\left(\frac{T_c}{100}\right)^4 = 78.86$	$\left(\frac{T_c}{100}\right)^4 = 8.22$
$\dot{Q}_i = -35$ W	$\dot{Q}_i = -15$ W
$A = 0.31$ m^2	$A = 0.31$ m^2
$\sigma = 5.67$	$\sigma = 5.67$
$F = 0.12$	$F = 0.61$
Louver blade opening angle $< 5°$	Louver blade opening angle $\geq 80°$

TABLE I. HEAT BALANCE ANALYSIS OF PEGASUS LOUVERS
(Continued)

PEGASUS II

"Cold" Case (June 12, 1965)	"Hot" Case (July 16, 1965)
$\left(\frac{T_s}{100}\right)^4 = 37.42$	$\left(\frac{T_s}{100}\right)^4 = 47.19$
$\left(\frac{T_c}{100}\right)^4 = 81.27$	$\left(\frac{T_c}{100}\right)^4 = 91.76$
$\dot{Q}_g = 45$ W	$\dot{Q}_g = 58.5$ W
$\dot{Q}_i = -35$ W	$\dot{Q}_i = 15$ W
F = 0.13	F = 0.54
Louver blade opening angle < 5°	Louver blade opening angle ≥ 70°

TABLE I. HEAT BALANCE ANALYSIS OF PEGASUS LOUVERS
(Concluded)

PEGASUS III

"Cold" Case (Sept. 29, 1965)	"Hot" Case (Aug. 25, 1965)
$\left(\frac{T_s}{100}\right)^4 = 35.44$	$\left(\frac{T_s}{100}\right)^4 = 43.4$
$\left(\frac{T_c}{100}\right)^4 = 76.76$	$\left(\frac{T_c}{100}\right)^4 = 82.09$
$\dot{Q}_g = 44$	$\dot{Q}_g = 48.5$
$\dot{Q}_i = -35$	$\dot{Q}_i = -35$ W
$F = 0.08$	$F = 0.5$
Louver blade opening angle < 5°	Louver blade opening angle ≥ 70°

TABLE II

RANGE OF PEGASUS TEMPERATURES

Component	Design Range (°K)	Actual Range (°K)
Pegasus I		
Radiation Detector	222 to 388	230 to 320
Batteries	272 to 322	300 to 305
Other Electronics	262 to 332	285 to 290
Solar Panels	194 to 339	215 to 345
Meteoroid Detect. Panels	167 to 394	215 to 370
Pegasus II		
Radiation Detector	222 to 388	240 to 295
Batteries	272 to 322	295 to 310
Other Electronics	262 to 332	285 to 325
Solar Panels	194 to 339	230 to 340
Meteoroid Detect. Panels	167 to 394	210 to 370
Pegasus III		
Radiation Detector	222 to 388	240 to 310
Batteries	272 to 322	295 to 300
Other Electronics	262 to 332	285 to 325
Solar Panels	194 to 339	235 to 310
Meteoroid Detect. Panels	167 to 394	220 to 350

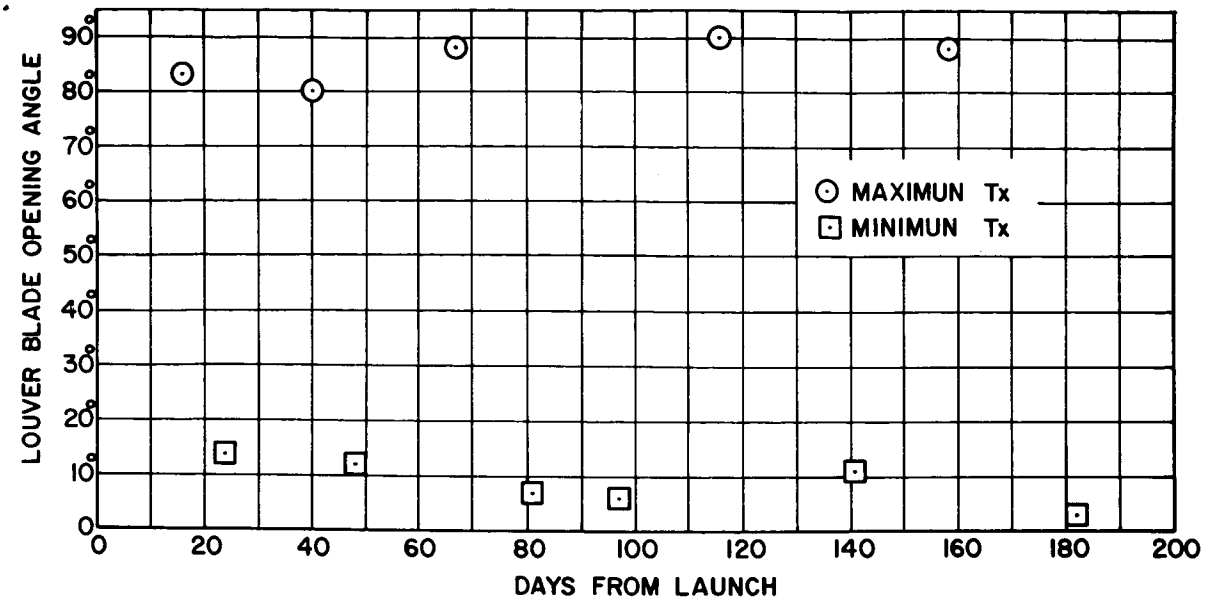

FIGURE 18. PEGASUS I LOUVER BEHAVIOR

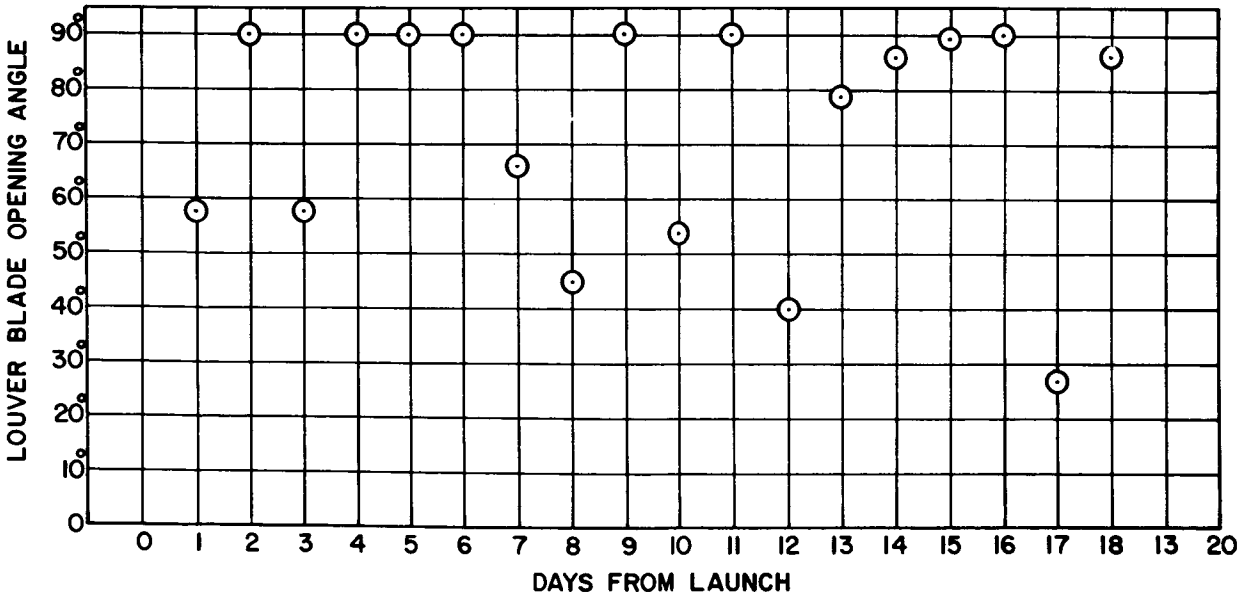

FIGURE 19. PEGASUS II LOUVER BEHAVIOR

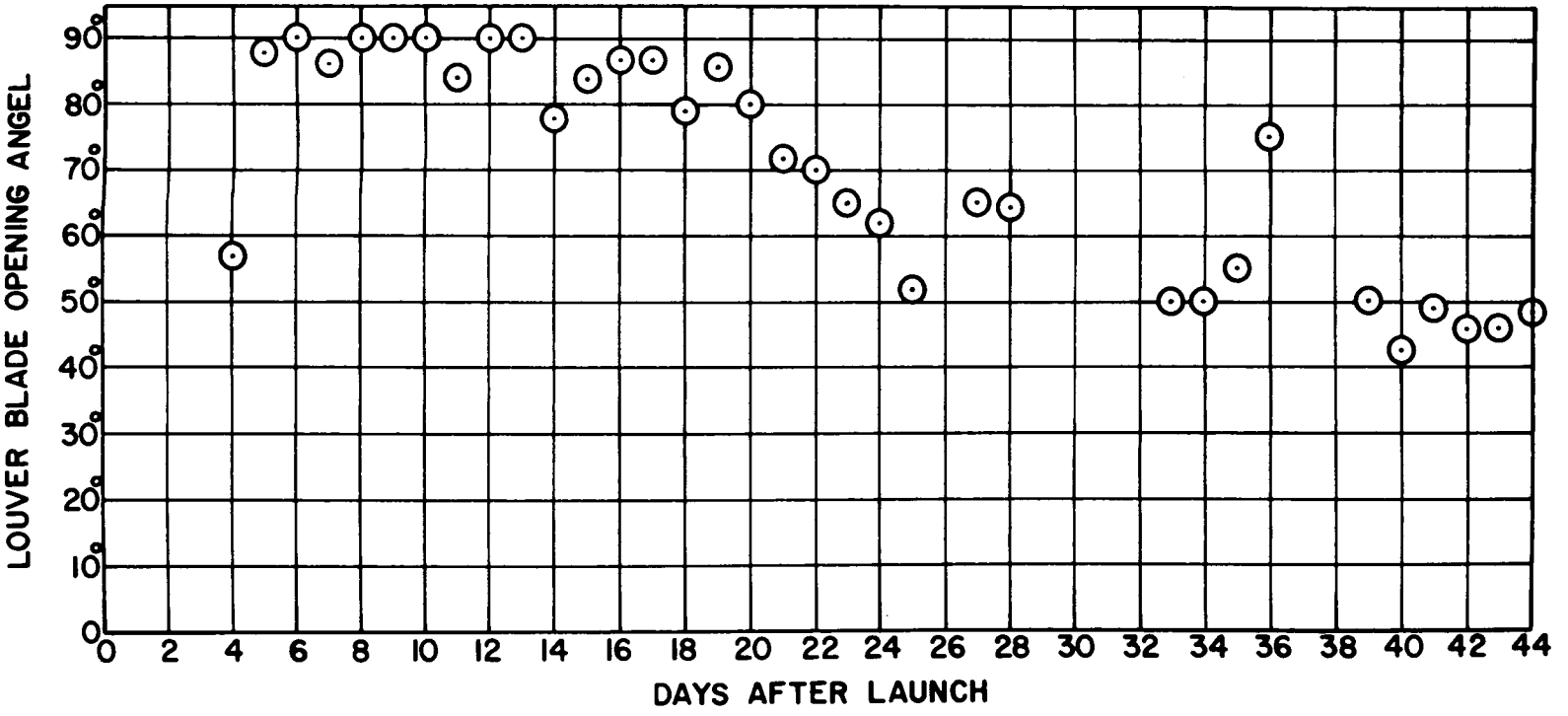

FIGURE 20. PEGASUS III LOUVER BEHAVIOR

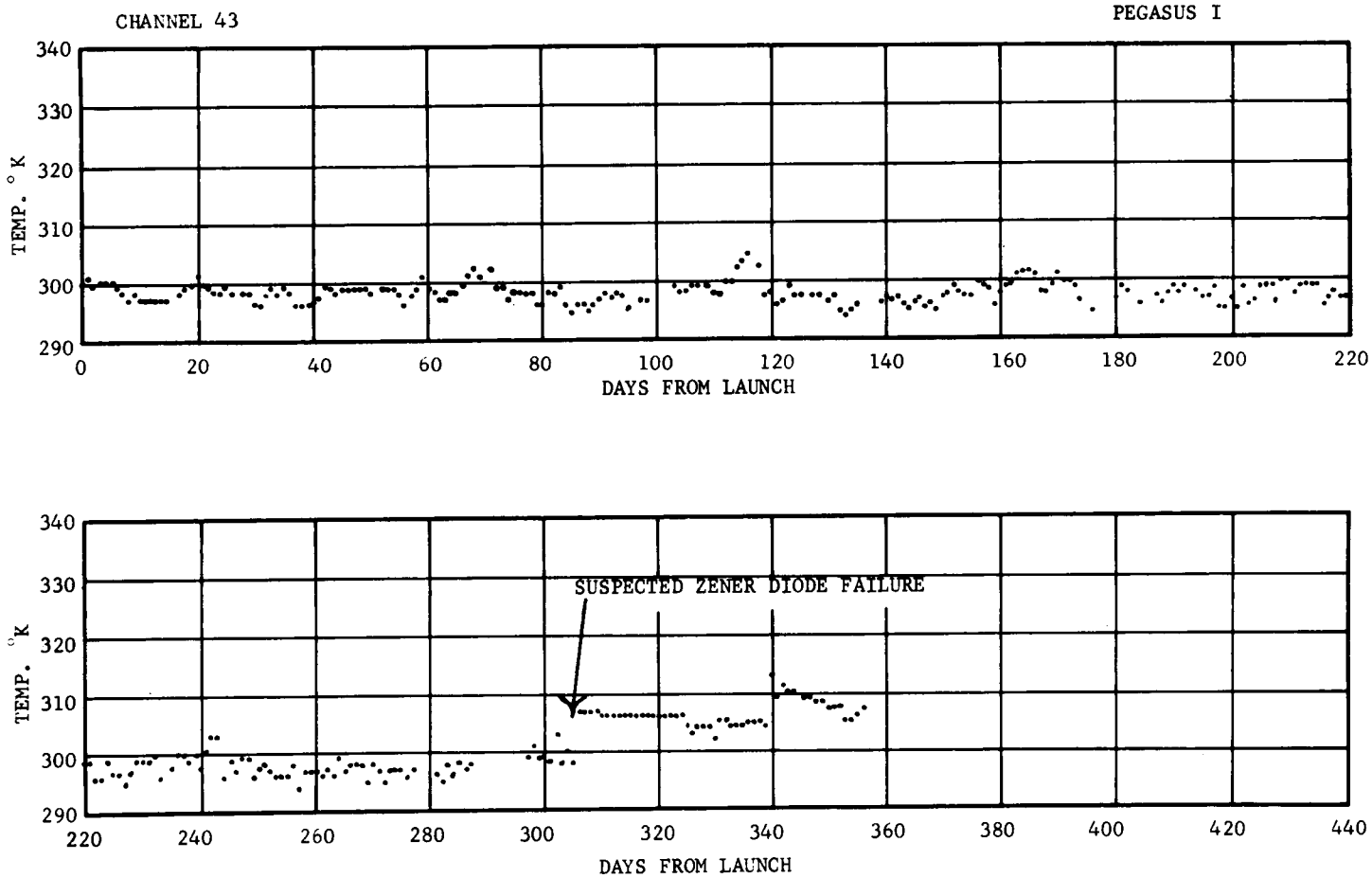

FIGURE 21. INTERNAL BATTERY TEMPERATURE - PEGASUS I

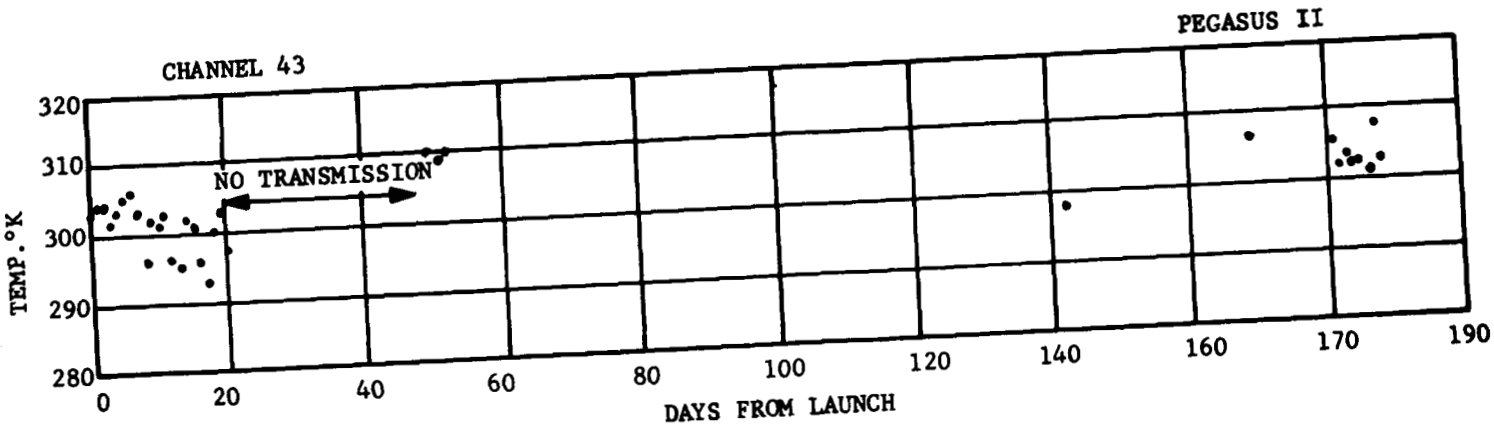

FIGURE 22. INTERNAL BATTERY TEMPERATURE - PEGASUS II

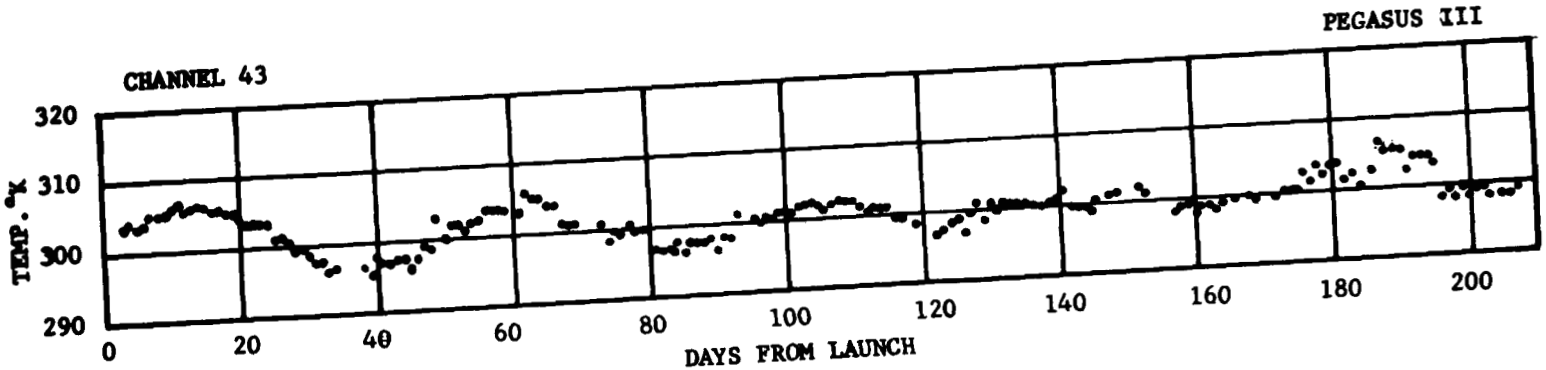

FIGURE 23. INTERNAL BATTERY TEMPERATURE - PEGASUS III

THERMAL STABILITY OF THE DETECTOR PANELS

The principal mission of the Pegasus spacecraft was to further define the micrometeoroid density in near-earth orbits, a task accomplished by the use of a very large "cross-section" (200 m^2) consisting of two extended wings of inter-connected capacitors. These large capacitors (Fig. 24) are discharged upon a micrometeoroid penetration; this event is coded electronically and transmitted to ground stations by telemetry. The penetration frequency is determined by the number of events recorded for a given capacitor plate thickness in an arbitrary time period. The principal object of the detector panel's thermal design was to maintain the temperatures within the range 167° K to 394° K, with a $\dot{T}$ less than 100° K/min.

The thermal control coating selected for the panels was a light-green substance called Alodine. Alodine refers to the chemical conversion of aluminum and aluminum alloy surfaces to $CrPO_4$, $AlPO_4$, and water, with trace elements of fluorides. The thinness of the Alodine coating required to obtain the desired optical and thermal properties, negligibly altering the micrometeoroid penetration properties, was the deciding factor in its selection.*

Extensive and comprehensive preflight studies were conducted to define the radiometric properties of Alodine and to determine its stability in a simulated space environment. Using a thermal environment space chamber at R-RP-T, a full-sized detector panel was instrumented with four strategically located thermocouples and subjected to cyclic temperature variations to determine the heat flow characteristics. A small contract let to Lockheed (Palo Alto, Calif.) indicated the Alodine coating was exceptionally stable to ultraviolet irradiation. A brief summary of on-the-pad radiometric measurements of the detector panels is given in Table III. The main objectives of this postflight analysis were to determining the degree of conformity with thermal design specifications of the panels and to determine the relative stability to ultriviolet irradiation of the Alodine coating.

---

* Slight modifications to the chemical bath, initiated to lower the α/ϵ ratio of the resultant coating, induced the prime contractor, Fairchild-Hiller Corporation, to designate the process as MTL-3.

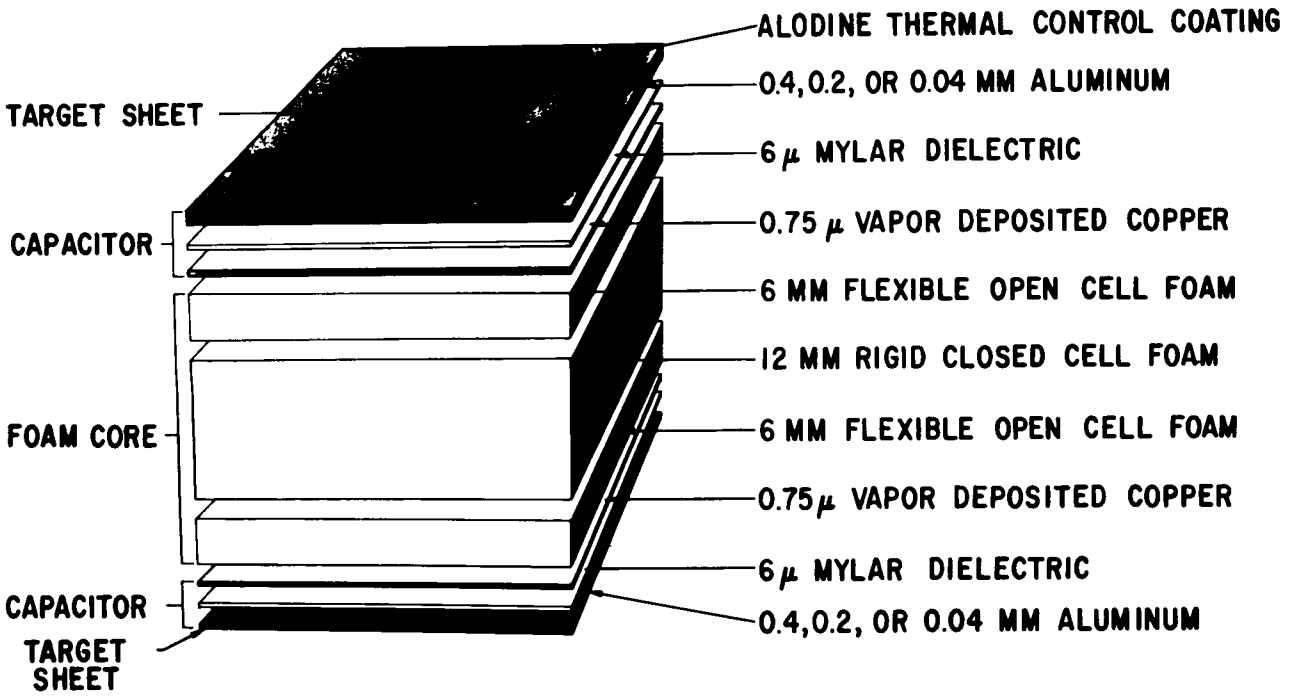

FIGURE 24. METEOROID SENSOR PANEL (EXPLODED VIEW)

TABLE III. SUMMARY OF ON-THE-PAD RADIOMETRIC SURVEY ON PEGASUS I

I.	Measurements made on Alodine (MTL-3) coated tabs placed near Pegasus (1) $0.51 \leq \alpha_s \leq 0.53$ (2) $0.53 \leq \epsilon_N \leq 0.58$ (3) $\alpha_s/\epsilon_N \leq 1.0$
II.	Measurements made on the detector panels (1) $0.50 \leq \alpha_s \leq 0.56$ (2) $0.53 \leq \epsilon_N \leq 0.65$ (3) $\alpha/\epsilon \leq 1.0$

α_s measurements were made with a portable Gier-Dunkle reflectometer.

ϵ_N measurements were made with portable Lions emittometer.

RESULTS

The results of this study apply, in actuality, only to a small, 15.24 by 15.24-cm (6 by 6-in.), simulated detector panel placed above the +Y "wing" side in the X-Y plane (see Fig. 11). The Alodine coating for this panel was prepared in the same manner as for the full-sized detector panels. Unfortunately, because of inaccessibility of this panel when positioned, no radiometric measurements were performed. As a result, postlaunch evaluation of detector panel temperatures provides only a basis for comparison. That is, if coating degradation is discovered, it can only be assumed that the detector

panels themselves have degraded an equivalent amount. The temperature of the dummy panel is monitored on both the +Z and -Z sides, thus providing a method for evaluating performance for both sides independently.

A computer program, adapted from the General Space Thermal Program was developed to compute a thermal history of the Pegasus I dummy panels for a given time interval. The basic equations (Appendix) were utilized in a four-node analysis, thus introducing four simultaneous differential equations to be solved * (Fig. 25). The equations were somewhat simplified because of the negligible magnitude of the parameters R_{ij} and $\dot{Q}_i$. The simplification resulted from the total omission of these parameters in the program itself, a justifiable approximation when the relative magnitudes of all parameters are considered. The program was run on an IBM 7094 computer producing both tabular printout and graphical representation of the resulting data. Computed thermal histories, usually encompassing two or three orbits, were compared to Pegasus orbital data stored on microfilm to determine the curve similarity. Close theoretical curve fits to orbital data thus supplied the magnitudes of various detector panel parameters, particularly the solar absorptance (α_s) and infrared emittance (ϵ_{ir}).

The time interval of Pegasus I selected as a basis of comparison for a given computer run was usually selected on the basis of available attitude data. This limited the analysis to the period March 9 through May 7, 1965; as a result, thermal design evaluation of the detector panels was extended past May only by comparison of orbital temperature data for orbits with similar MAS angles. Results of this type of study are considered in more detail later in this report.

Two plots obtained from the thermal analysis computer program are shown in Figures 26 and 27, with the PCM data curves included for comparison. It is obvious from a comparison of these figures that the degradation of the Alodine coating is small; the value of α/ϵ is shown for comparison on the respective graphs. These two curve-fits are typical of the many that were generated for Pegasus I in the period March through May 1965; it is concluded that the Alodine coating has undergone less than five percent degradation in this period.

---

* The quantity of nodes chosen is arbitrary.

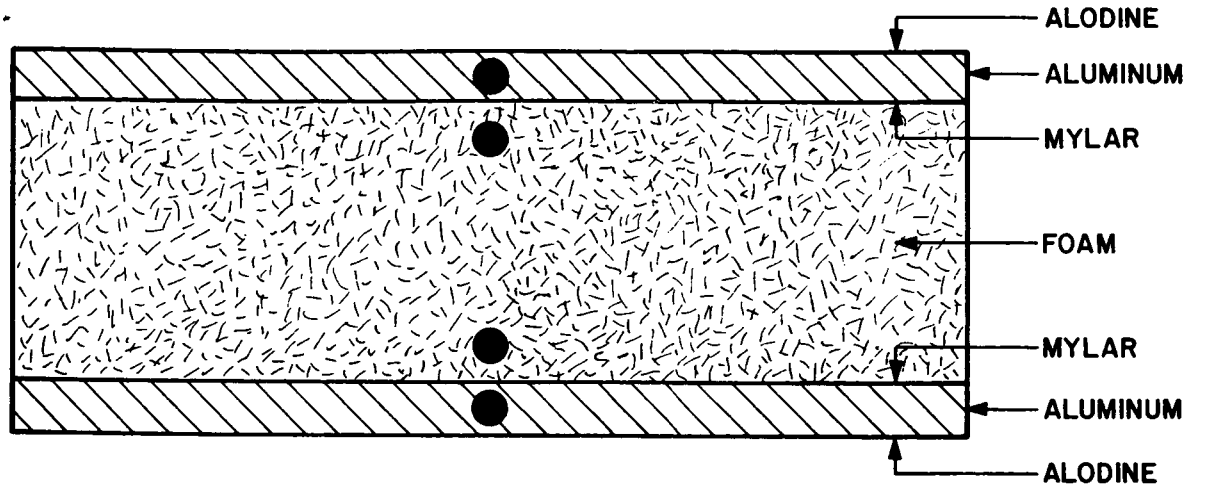

FIGURE 25. CROSS-SECTIONAL VIEW OF PEGASUS MICROMETEOROID DETECTOR PANEL SHOWING THERMAL NODES

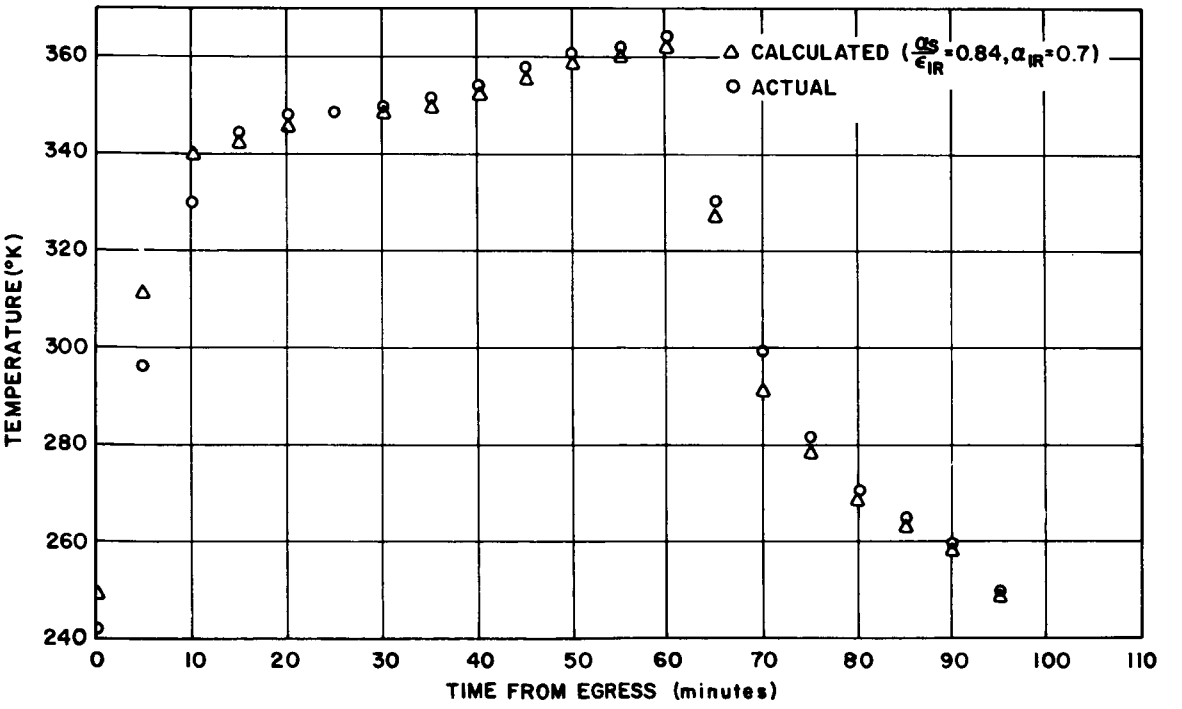

FIGURE 26. PEGASUS I DETECTOR PANEL TEMPERATURES (MARCH 20, 1965)

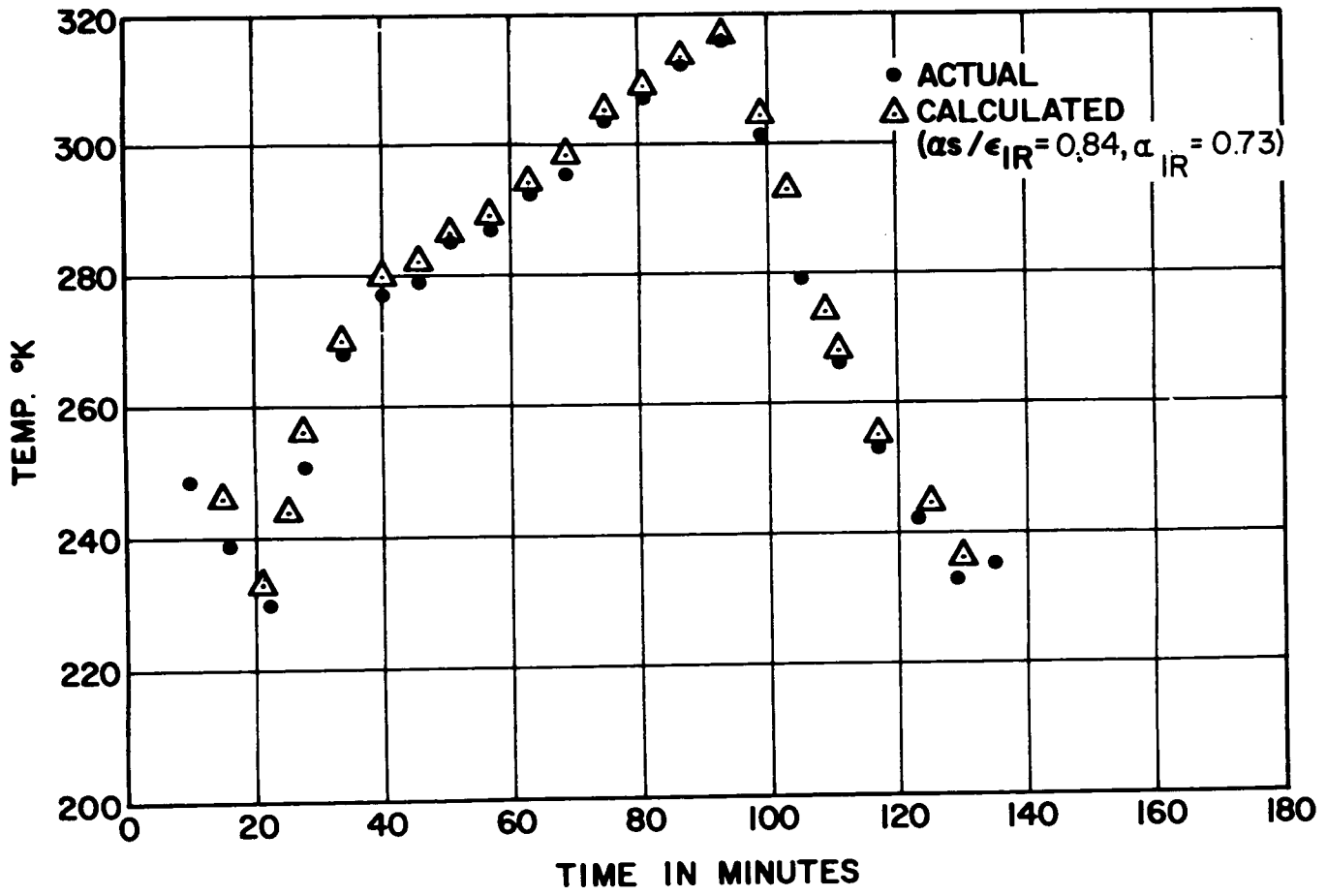

FIGURE 27. PEGASUS I DETECTOR PANEL TEMPERATURES (APRIL 21, 1965)

The complicated motion of Pegasus II and III has caused endless difficulty in the thermal design evaluation. To determine the stability of the Alodine coating on the two vehicles, the only available method of analysis consists of comparing PCM temperature data with the thermal design tolerances. This approach, after careful study of a great number of curves, has led to the conclusion illustrated by the curves shown in Figure 28; that is, the similarity with Pegasus I panel temperatures is very close on the average and the upper and lower design tolerance have not been reached. The Alodine coating for the detector panels of Pegasus II and of Pegasus III has undergone little, if any, degradation, and has withstood the rigors of the space environment equally as well as Pegasus I since no upward or downward trends in the panel temperatures as a whole have been observed. The thermal design of the Pegasus detector panels was very successful indeed.

The method for determining the long-term stability of the Alodine coating was approached in a different manner than that previously described A scan of Pegasus I attitude data produced several widely separated time intervals when the attitude was similar. This insures a high degree of similarity in the thermal environment for the two periods. The temperature curves were then compared to determine any difference, which would, if discovered, indicate some degradation of the Alodine coating. This analysis extended the period of Pegasus I available for study up through November 1965. The results (Figs. 29 and 30) indicate the Alodine has degraded very little, if at all.

George C. Marshall Space Flight Center
National Aeronautics and Space Administration
Huntsville, Alabama, October 6, 1966

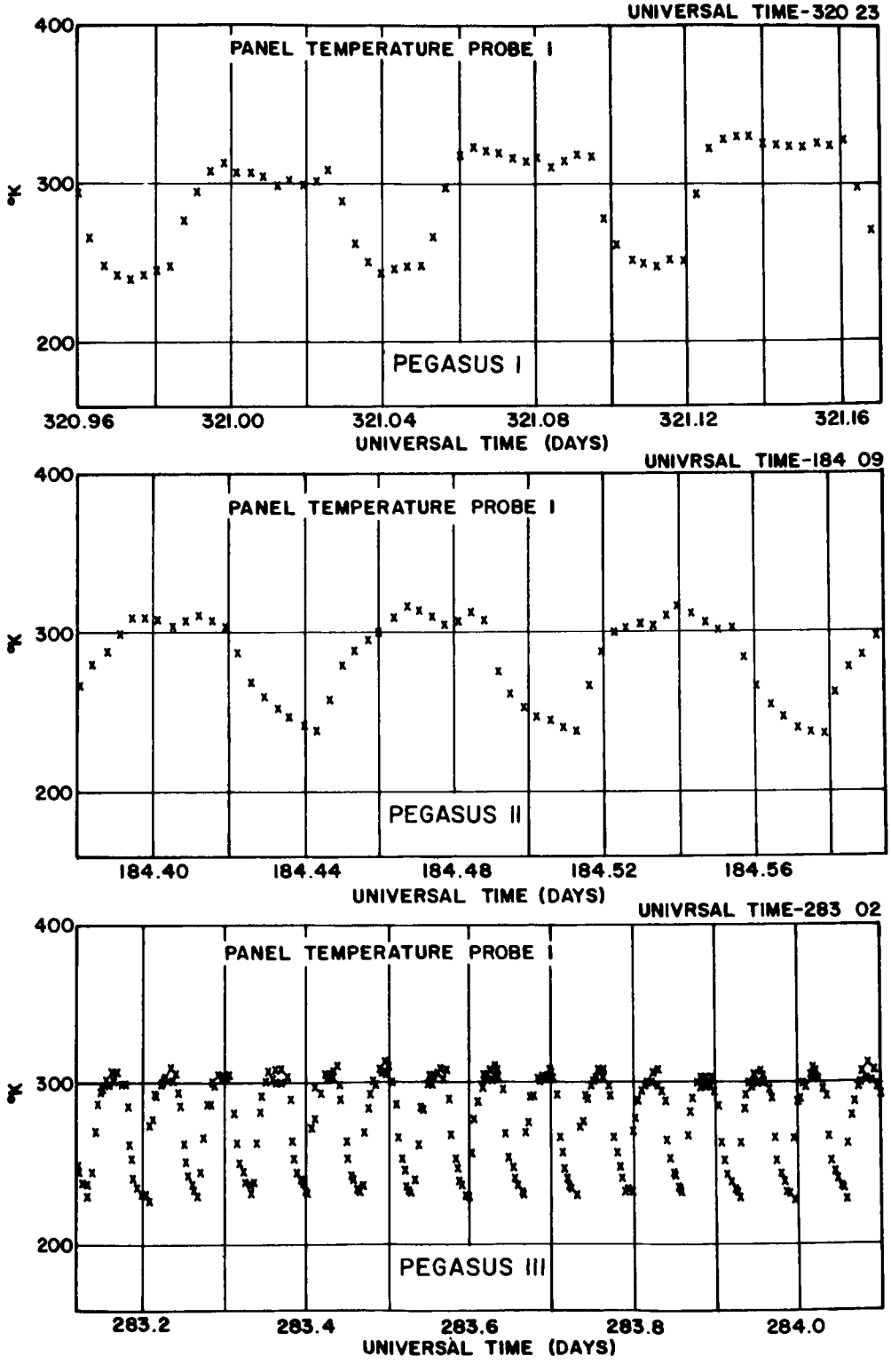

FIGURE 28. PEGASUS I, PEGASUS II, PEGASUS III PANEL TEMPERATURE PROBES

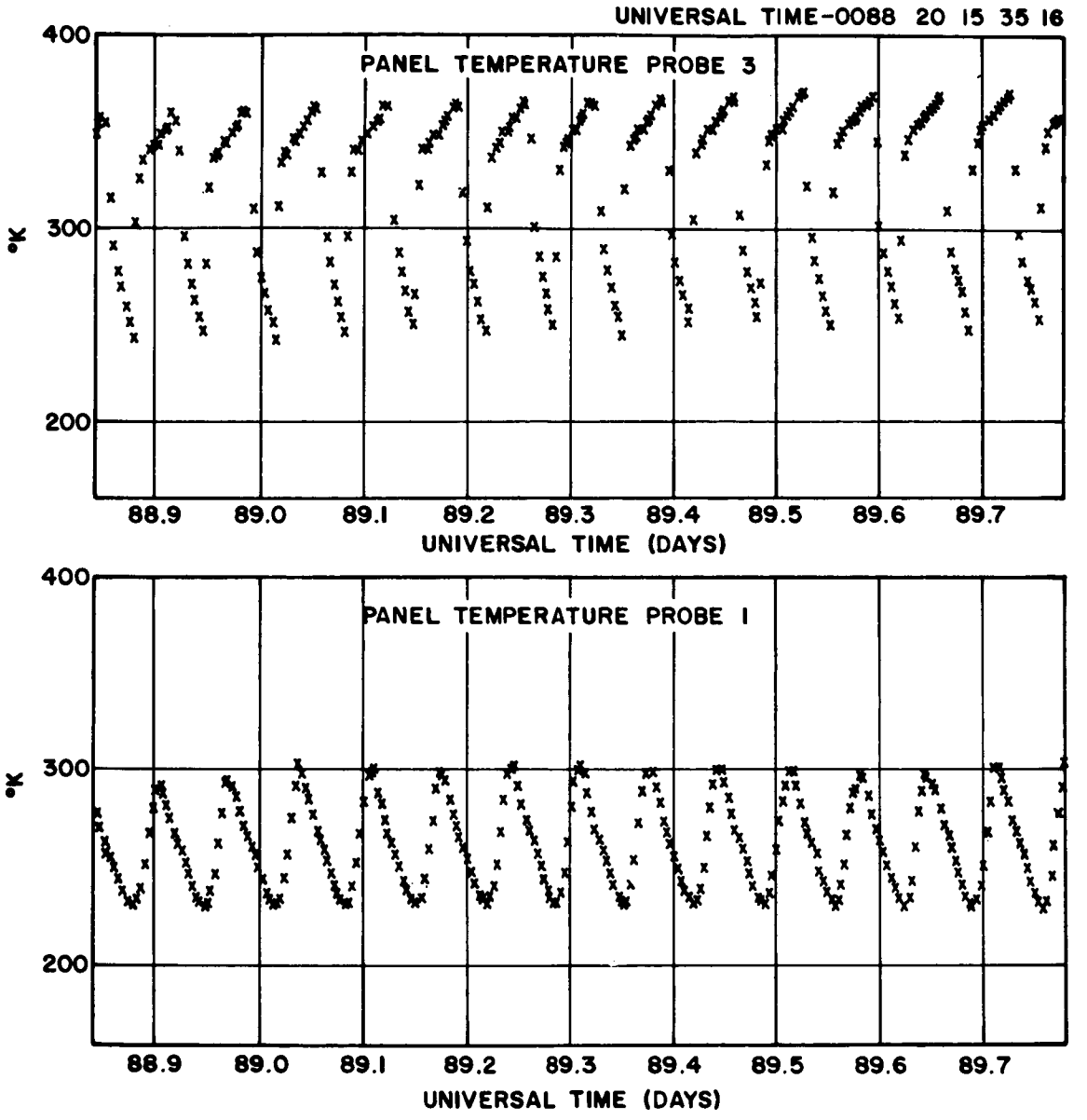

FIGURE 29. PEGASUS I PANEL TEMPERATURES WITH MAS = 125°

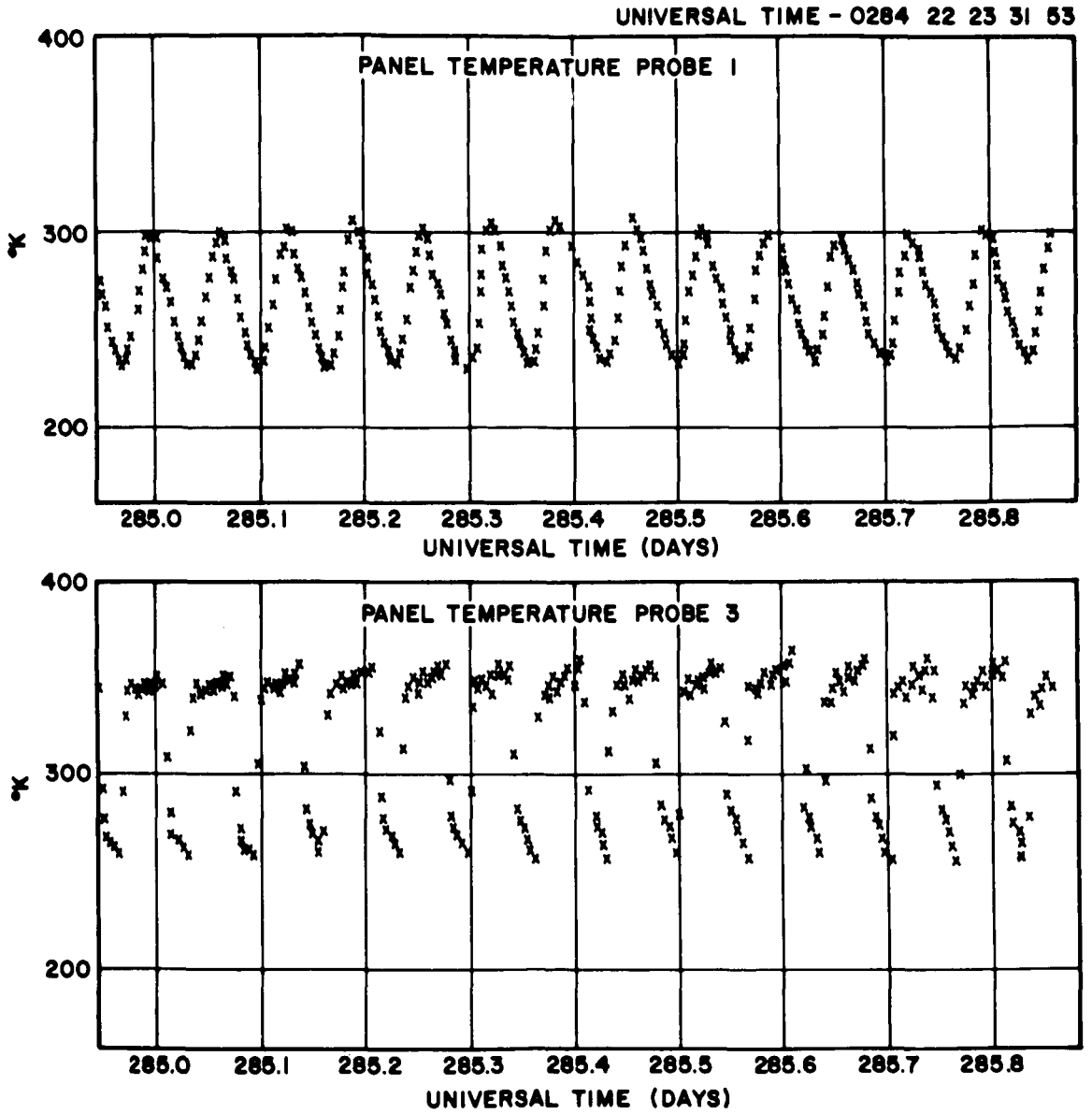

FIGURE 30. PEGASUS I PANEL TEMPERATURES WITH MAS = 125°

APPENDIX. THE GENERAL SPACE THERMAL PROGRAM*

This program includes subroutines for obtaining geometric and orbital parameters necessary to compute the many flux terms, and, simultaneously, solves a set of "n" calorimetric equations of the general form:

$$\dot{T}_i H_i = A_{1i}\,\alpha_i\,S + A_{2i}\,\alpha_i\,SB + A_{3i}\,\epsilon_i\,SE - A_{4i}\,\epsilon_i\,\sigma\left(\frac{T_i}{100}\right)^4 + \sum_{j=1}^{n}\left[C_{ij}\,T_j + R_{ij}\left(\frac{T_j}{100}\right)^4\right] - T_i\sum_{j=1}^{n} C_{ij} - \frac{T_i}{100}\sum_{j=1}^{n} R_{ij} + \dot{Q}_i$$

where

T_i = temperature of node i

$\dot{T}_i = \frac{dTi}{dt}$

H_i = heat cap of node i

C_{ij} = conductance between nodes i and j

R_{ij} = radiance between nodes i and j

$\dot{Q}_i$ = internal heat of node i

---

* The general computer program was developed by Research Projects Laboratory (-T) and Computation Laboratory (-P).

$\overline{\cos RAS} = \frac{\cos \delta}{\pi}$, where δ is the angle between the orbital plane and the ascending node of the satellite.

T_x = percent time in sunlight

α_1 = solar absorptance node i

ϵ_1 = IR emittance of node i

S = solar constant (1400 watts/m^2)

B = max % of S for albedo

E = max % of S for earth's IR

σ = Stefan-Boltzmann constant = 5.67 joules/deg K

A_{1i} = area function for incident solar energy to node i

A_{2i} = area function for incident albedo energy to node i

A_{3i} = area function for incident earth IR to node i

A_{4i} = radiating area of node i

REFERENCES

1. Bannister, Tommy C., and Eby, Robert J.: Pegasus Thermal Design. NASA TN D-3625, Nov. 1966.

2. Bannister, T. C., and Schafer, C. F., Pegasus Thermal Control Coatings Experiment, AIAA Paper No. 66-419, AIAA 4th Aerospace Sciences Meeting, Los Angeles, Calif., June 27-29, 1966.

3. Naumann, R. and Mynatt, Amanda: Projected Area for a Tumbling Cylinder, R-RP, No. DV-TN-1-59, Feb. 1959.

4. Bannister, T. C.: Radiation Geometry Factor Between Earth and a Satellite. NASA TN D-2750, July 1965.

5. Solar-Radiation-Induced Damage to Optical Properties of ZnO-Type Pigments, NAS 8-11266, Lockheed Missiles and Space Co., Sept. 1965, Sunnyvale, Calif.

6. Plamandon, J. A.: Analysis of Movable Louvers for Temperature Control. JPL Tech Report No. 32-555, Jan. 1, 1964.

"The aeronautical and space activities of the United States shall be conducted so as to contribute . . . to the expansion of human knowledge of phenomena in the atmosphere and space. The Administration shall provide for the widest practicable and appropriate dissemination of information concerning its activities and the results thereof."

—NATIONAL AERONAUTICS AND SPACE ACT OF 1958

NASA SCIENTIFIC AND TECHNICAL PUBLICATIONS

TECHNICAL REPORTS: Scientific and technical information considered important, complete, and a lasting contribution to existing knowledge.

TECHNICAL NOTES: Information less broad in scope but nevertheless of importance as a contribution to existing knowledge.

TECHNICAL MEMORANDUMS: Information receiving limited distribution because of preliminary data, security classification, or other reasons.

CONTRACTOR REPORTS: Technical information generated in connection with a NASA contract or grant and released under NASA auspices.

TECHNICAL TRANSLATIONS: Information published in a foreign language considered to merit NASA distribution in English.

TECHNICAL REPRINTS: Information derived from NASA activities and initially published in the form of journal articles.

SPECIAL PUBLICATIONS: Information derived from or of value to NASA activities but not necessarily reporting the results of individual NASA-programmed scientific efforts. Publications include conference proceedings, monographs, data compilations, handbooks, sourcebooks, and special bibliographies.

Details on the availability of these publications may be obtained from:

SCIENTIFIC AND TECHNICAL INFORMATION DIVISION

NATIONAL AERONAUTICS AND SPACE ADMINISTRATION

Washington, D.C. 20546